The Abdus Salam
International Centre for Theoretical Physics

United Nations
Educational, Scientific and
Cultural Organization

IAEA
International Atomic Energy Agency

2060-19

Advanced School on Non-linear Dynamics and Earthquake Prediction

28 September - 10 October, 2009

Reverse Tracing of Precursors within Earthquake Chains

P. Shebalin
International Institute of Earthquake Prediction Theory
& Mathematical Geophysics
Moscow
Russia

shebalin@mitp.ru/shebalin@ipgb.jussieu.fr

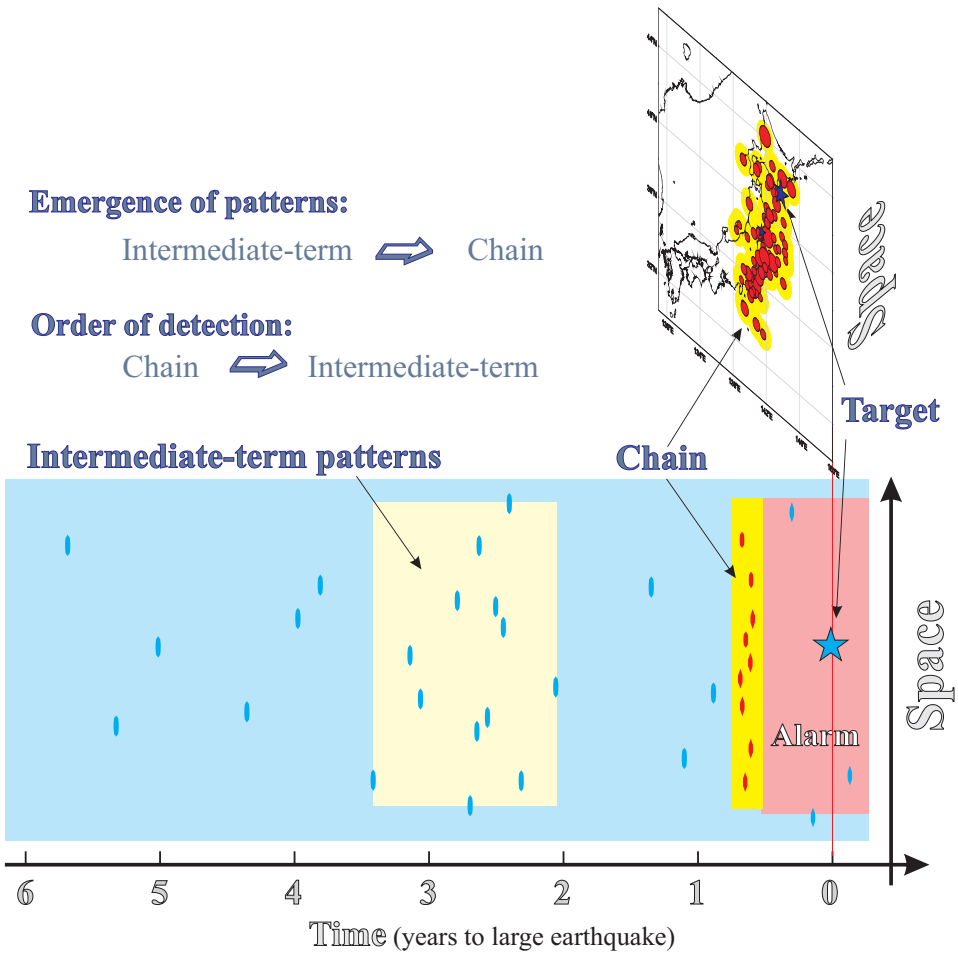

Reverse Tracing of Precursors (RTP)

Step 1. "Earthquake chain" depict an area of a long-range short-term activation of seismicity. As a rule, large earthquakes are preceded by earthquake chains. Not all chains precede large earthquakes, hence the Step 2 is needed to eliminate false alarms.

Step 2. In an area depicted by earthquake chain we analyze intermediate-term precursors, combining them using pattern recognition approach. By the mean of massive retrospective tests we estimate the probability of a false alarm. In case this probability is estimated to less than 50%, we set up in this area prediction of a large earthquake for a period of few months.

What are the advantages of *RTP*?

Hypothesis 1:
shorter-term pattern (chain) geometrically correlates with intermediate-term patterns.

RTP gives reduction in dimensionality of parameter space where premonitory patterns are looked for.

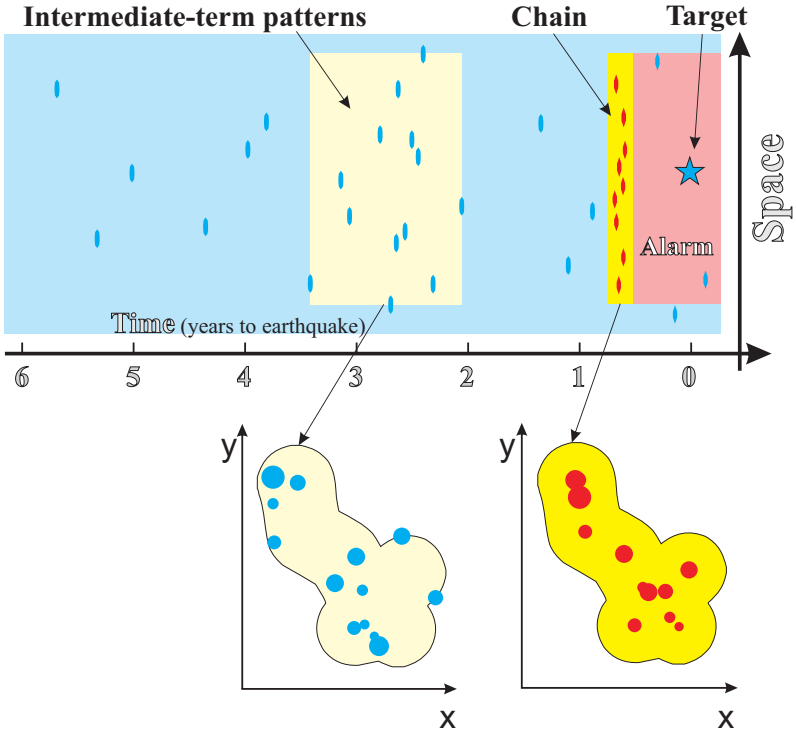

If circles, what size?

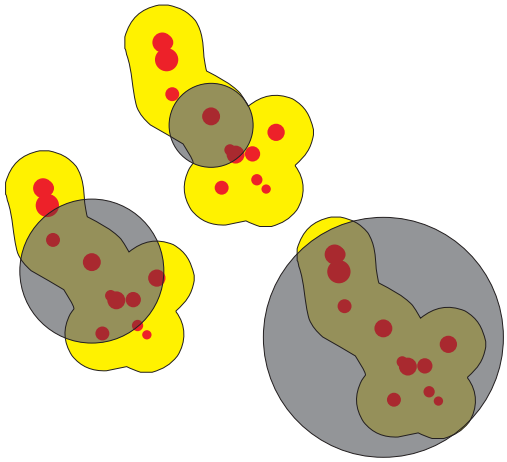

Hypothesis 2:
Chains are self-adapted to size and form of the area where precursors emerged

Intermediate-term patterns

considered in the R-vicinity of the chain

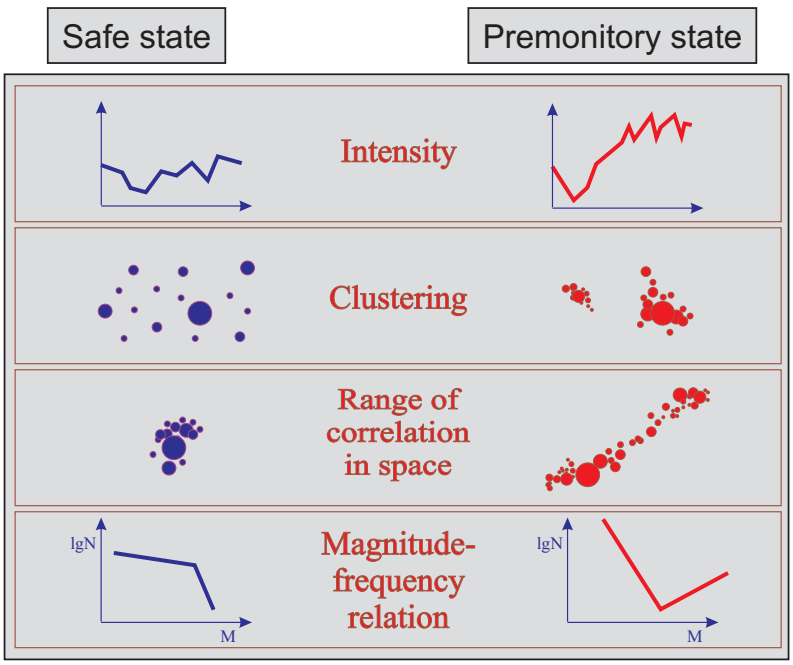

- Benioff strain release
- Total area of faultbreaks
- Number of earthquakes

[KB & Malinovskaya 1964; Bufe & Varnes,1993; Bowman et al.,1998; Knopoff et al., 1996; Jaume & Sykes,1999]

- Burst of immediate aftershocks
- Swarms of mainshocks

[KB, Knopoff , Rotwain,1980; Molchan et al,1990]

- Accord: simultaneous activation of distant areas
- ROC: simultaneous occurrence of distant intermediate events

[Kossobokov, Carlson, 1995; Gabrielov et al., 2000; Shebalinet al., 2000; Zaliapin et al.,2002]

- Upward bend of GR law

[Narkunskaya Schnirman , 1990; Gabrielovet al., 2000; Zaliapin et al., 2003]

Intermediate-term premonitory seismicity patterns (lead time years) are studied in the *R*-vicinities of the ***Chains*** (lead time months). ***Pattern recognition*** is applied to select precursory chains. Available case histories are used for learning.

Functions F_p capturing different premonitory phenomena

We consider functions in ***time*** scale or in ***event*** scale.

Time scale: for the time t the value of the function $F_p(t)$ is calculated using information in the catalog in the interval (t-s, t).

Event scale: time is discrete, we consider only moments of the events. For the time t_j the value of the function $F_p(t_j)$ is calculated using events j-N,j-N+1,...,j.

All functions are normalized to the seismicity of the R-vicinity of the chain: events with M>=m* are considered;
m* is found to have n* events per year in the interval (t_{chain}-5 years,t_{chain}-1 year),
where t_{chain} - time of the first event in the chain.

8 sets of common parameters are used in ALL regions, 2 x 2 x 2: (*R*=100km and *n=20 or *R*=50km and *n**=10) x (*N*=20 or 50) x (T=0.5 year or 2 years); *r*=50 km**

Functions for intermediate-term patterns in time and event scales

Time scale	Event scale
Rise of activity: *1. Activity*	
$F_U(t,s)=\frac{N_{t-s\le t_k<t}}{s}$	$\tilde{F}_U(t_j,N)=\frac{N}{t_j-t_{j-N+1}}$
2. *Sigma*	
$F_\Sigma(t,s)=\log_{10}\sum_{t-s\le t_k<t}10^{M_k-M^*}$	$\tilde{F}_\Sigma(t_j,N)=\log_{10}\sum_{k=j-N+1}^{j}10^{M_k-M^*}$
3. *Rise of magnitudes*	
$F_M(t,s)=\frac{\sum M_k}{N_{t-\frac{s}{2}\le t_k<t}}-\frac{\sum M_k}{N_{t-s\le t_k<t-\frac{s}{2}}}$	$\tilde{F}_M(t_j,N)=\frac{2}{[N/2]}\left(\sum_{k=j-N+1}^{j-N+[N/2]}M_k-\sum_{k=j-[N/2]+1}^{j}M_k\right)$
4. Acceleration	
$F_C(t,s)=\frac{\sum\frac{1}{t_k-t_{k-1}}}{N_{t-\frac{s}{2}\le t_k<t}}-\frac{\sum\frac{1}{t_k-t_{k-1}}}{N_{t-s\le t_k<t-\frac{s}{2}}}$	$\tilde{F}_C(t_j,N)=\frac{1}{[N/2]}\left(\sum_{k=j-N+1}^{j-N+[N/2]}\frac{1}{t_k-t_{k-1}}-\sum_{k=j-[N/2]+1}^{j}\frac{1}{t_k-t_{k-1}}\right)$
Rise of clustering: *5. Swarm*	
$F_W(t,s)=1-\frac{A_r(t)}{\pi r^2 N_{t-s\le t_k<t}}$	$\tilde{F}_W(t_j,N)=1-\frac{A_r(t_j)}{\pi r^2 N}$
6. B-micro	
$F_{B_u}(t,s)=\log_{10}\sum_{t-s\le t_k<t}\sum_{l}10^{M_{kl}-M^*}$	$\tilde{F}_{B_u}(t_j,N)=\log_{10}\sum_{k=j-N+1}^{j}\sum_{l}10^{M_{kl}-M^*}$
Rise of earthquakes correlation range: *7. Accord*	
$F_A(t,N)=\tilde{F}_A(t_j,N)=\frac{A_r(t)}{\pi r^2}$	
Transformation of Gutenberg-Richter relation: *8. Gamma*	
$F_G(t,N)=\tilde{F}_G(t_j,N)=\frac{1}{N_{M_k\ge M_{1/2}}}\sum_{M_k\ge M_{1/2}}(M_k-M^*)$	

Pattern recognition: algorithm “Hamming distance”

Formally, the Hamming distance between two Boolean vectors of the same length is defined as the number of their non-coincident symbols. Here, the Hamming distance gives the number of emergent intermediate-term premonitory patterns.

Emergence of a pattern at the moment *t* is captured by the condition $F_P(t) \geq C_P$. Each threshold C_P is determined automatically at the learning stage. It minimises the sum *n* + *f*; here *n* is the rate of failures to predict and *f* is the rate of false alarms in prediction with a single pattern *P*.

Rise of activity: “Activity”

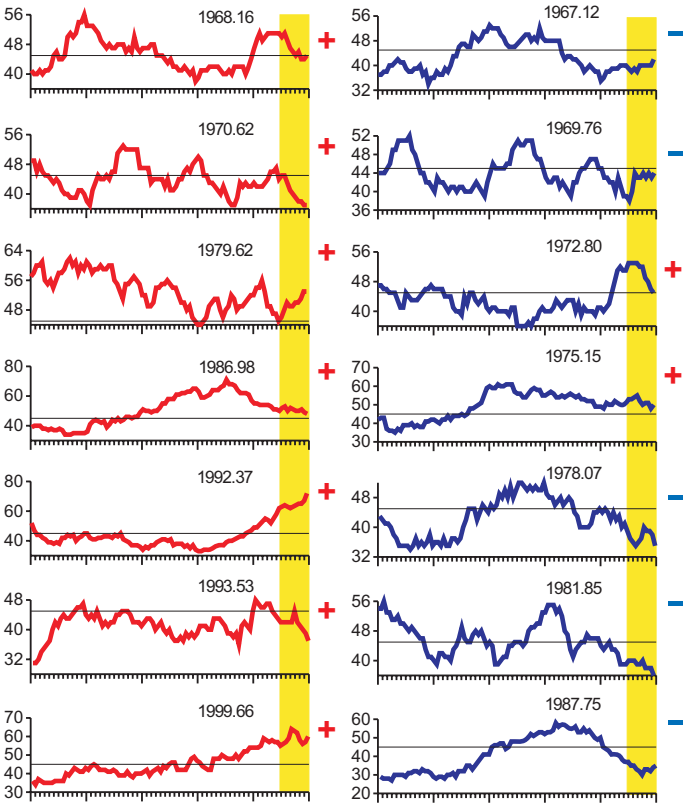

$$U(t_j) = \frac{N}{t_j - t_{j-N+1}}$$

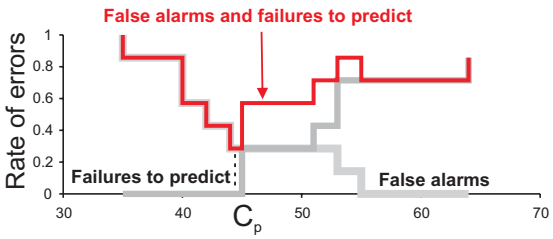

Rise of activity: “Sigma”

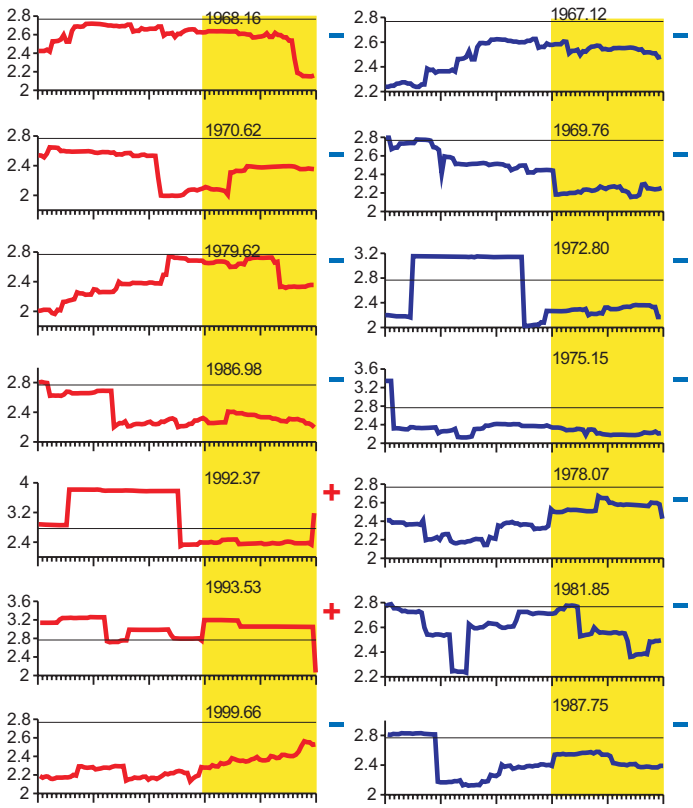

$$\Sigma(t_j) = \log_{10} \sum_{k=j-N+1}^{j} 10^{m_k} - m*$$

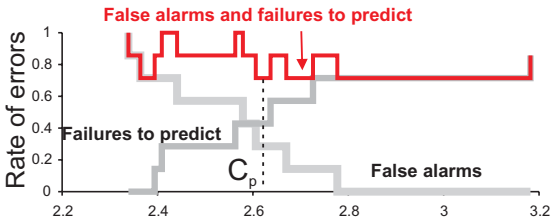

Rise of activity: “*Acceleration of number of earthquakes*”

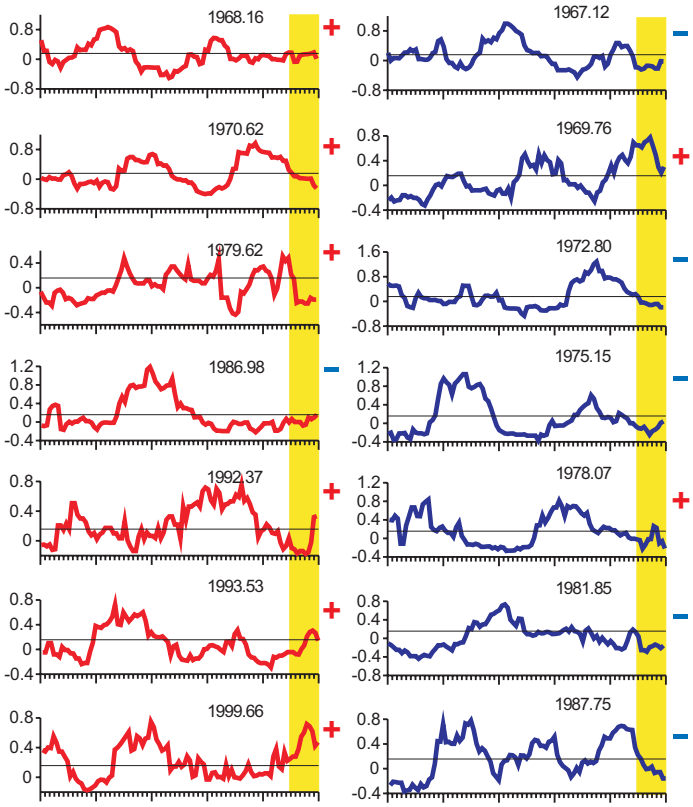

$$Acn(t_j) = \frac{2}{N}\{\sum_{k=j-[N/2]+1}^{j} \frac{1}{t_k - t_{k-1}} - \sum_{k=j-N+1}^{j-[N/2]} \frac{1}{t_k - t_{k-1}}\}$$

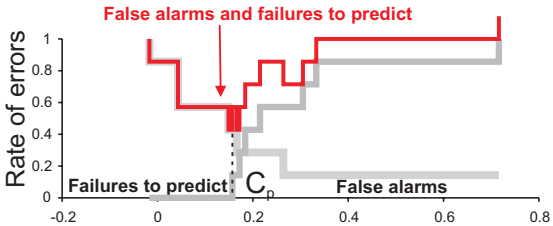

Rise of activity: “rise of magnitudes”

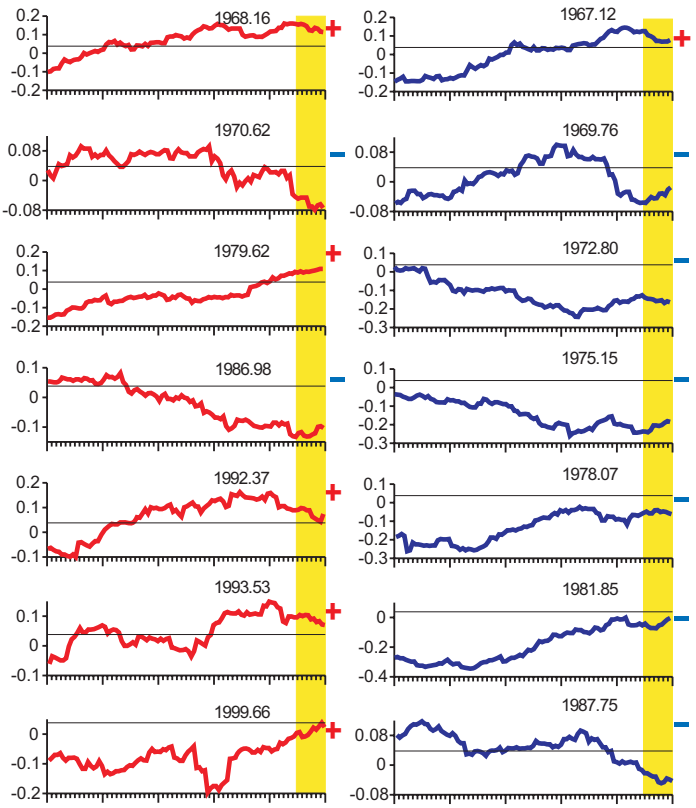

$$Acm(t_j) = \frac{2}{N}\{\sum_{k=j-[N/2]+1}^{j} m_k - \sum_{k=j-N+1}^{j-[N/2]} m_k\}$$

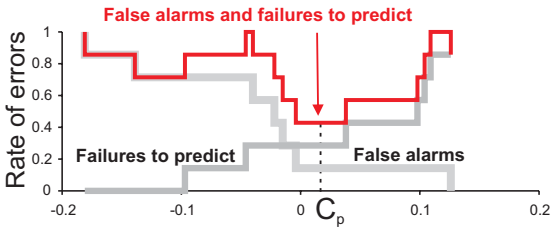

Rise of clustering: “Swarm”

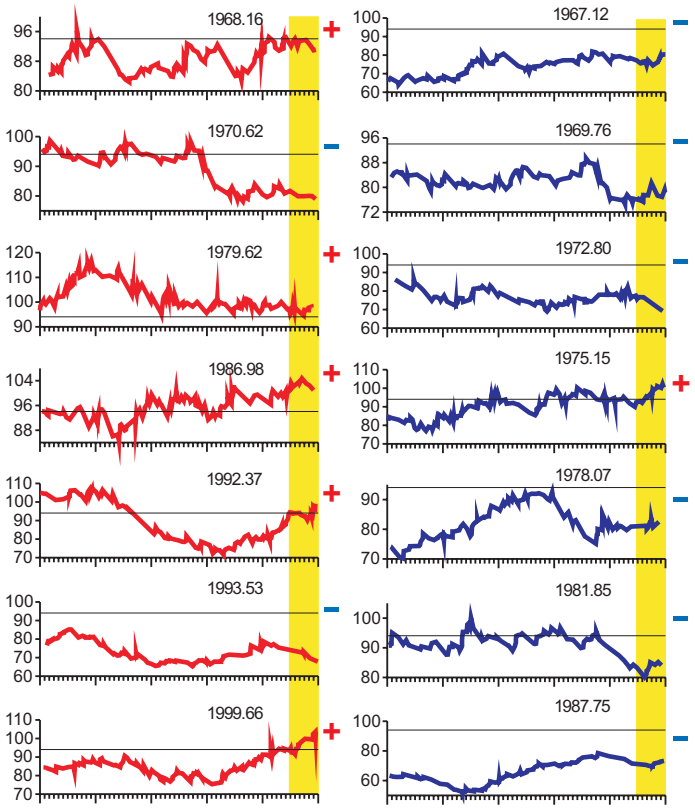

$$W(t_j) = \frac{A_r^{\cap}}{\pi r^2}$$

$A_r^{\cap}$ - total area of the intersection of at least two circles of radius r centered at N epicenters in the sequence; their sequence numbers are j-N+1, j-N+2,…,j.

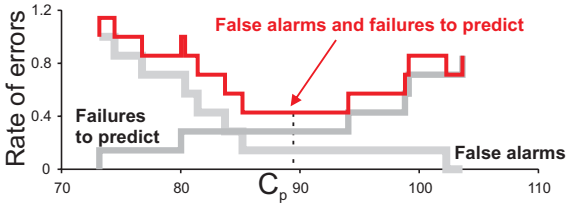

Rise of clustering: “b-micro”

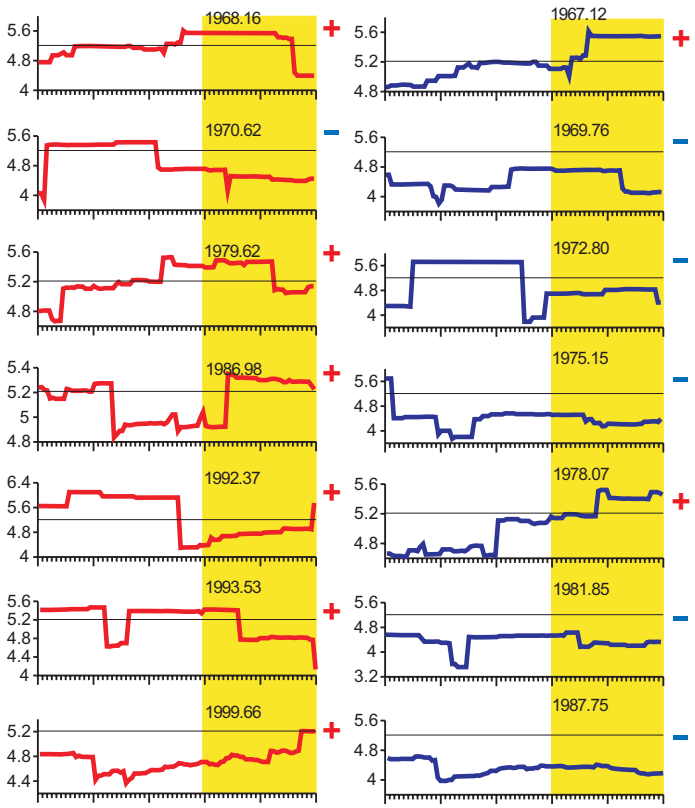

m_{kl} - magnitudes of the aftershocks during first two days after the k-th main shock, l = 1, 2,….;

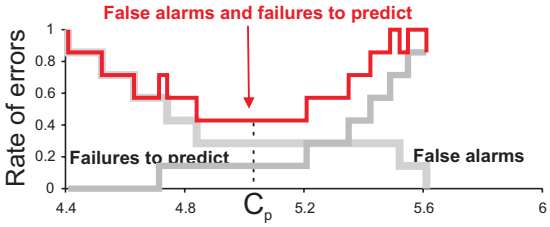

Rise of correlation range: “Accord”

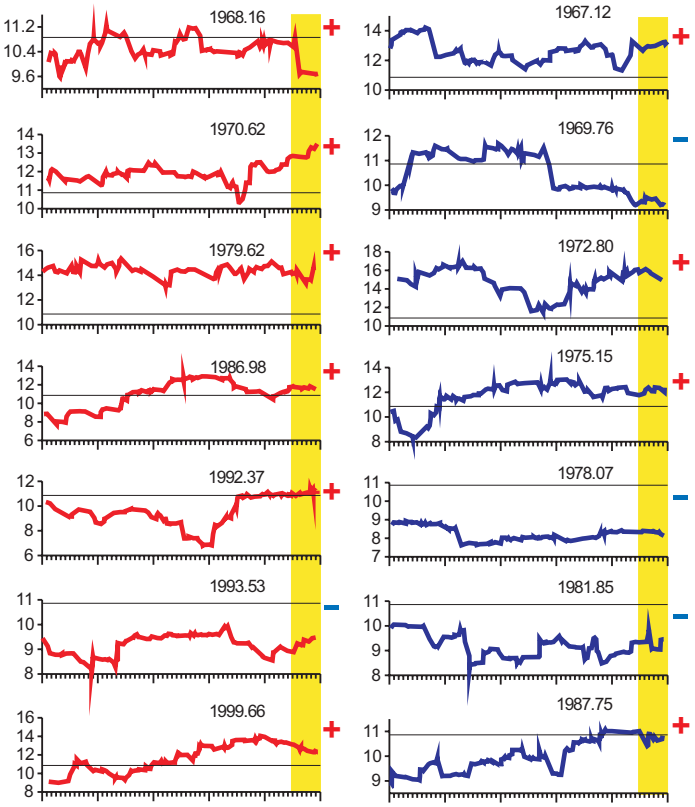

$$A(t) = \frac{A_r^{\cup}}{\pi r^2}$$

$A_r^{\cup}$ - area of the union of the circles of radius r centered at N epicenters in the sequence; their sequence numbers are j-N+1, j-N+2,…,j.

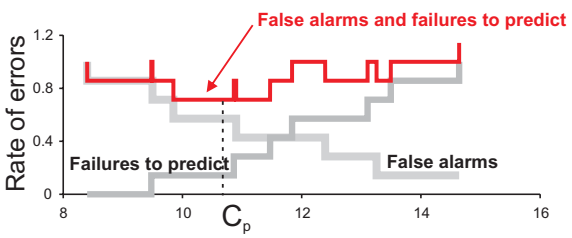

Transformation of Gutenberg-Richter relation: “Gamma”

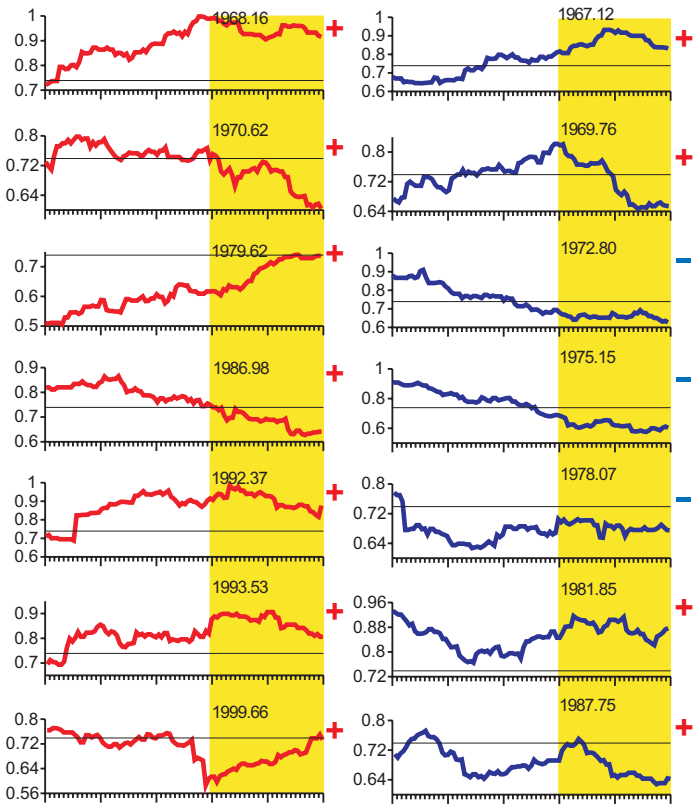

$$\gamma(t_j) = \frac{2}{N} \sum_{m_j \geq m_{1/2}} m_k$$

$m_{1/2}$ - median of magnitudes

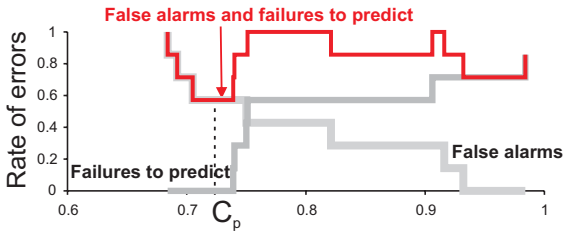

Choice of the radius *R* for the area of alarm

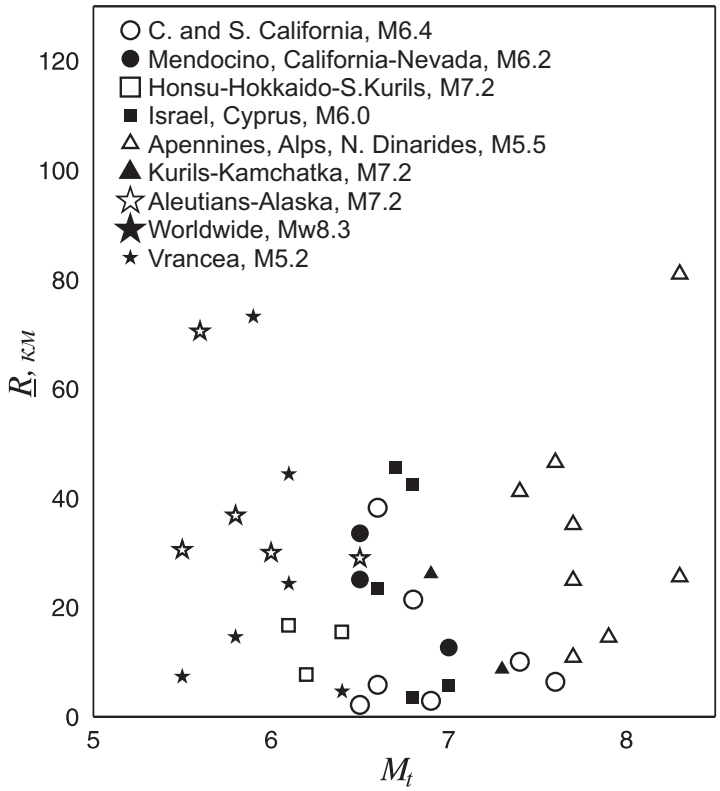

Final choice 100 km for targets M>=7.2, 50 km others.

Choice of the alarm duration

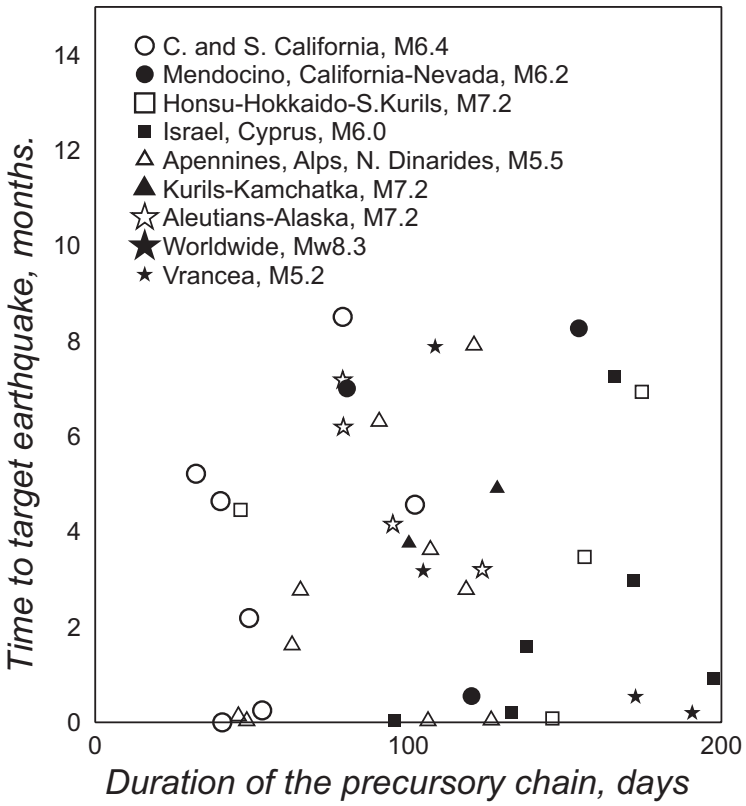

Final choice 9 months in all regions of the RTP test.

Step 1. The catalogue update

The area should be larger than the considered formal area to ensure correct aftershock elimination. Also this will help to avoid cutting chains extending across the formal boundaries (see below). We take two extra degrees of latitude and longitude to the area of consideration.

We use the following earthquake catalogues:

- California - ANSS composite catalogue

- Honshu-Hokkaido-S. Kuriles - JMA catalogue

- Apennines, Alps, N. Dinarides and Po Valley - NEIC/PDE

- Eastern Mediterrenian - the catalog of GII, Holon, Israel

- North Pacific (except Honshu-Hokkaido-S. Kuriles) - ANSS composite catalogue

Step 2. Aftershock elimination

The aftershocks are identified by the robust windowing with parameters according to Gardner-Knopoff [1974]. The catalogue of main shocks (aftershocks excluded) is then used; information about aftershocks that is used for the function "b-micro" (see below) is stored inside.

Magnitude of the main shock	Time window, days	Space window, km
M < 2.5	6	20
2.5 ≤ M < 3.0	11	23
3.0 ≤ M < 3.5	22	26
3.5 ≤ M < 4.0	42	30
4.0 ≤ M < 4.5	83	35
4.5 ≤ M < 5.0	155	40
5.0 ≤ M < 5.5	290	47
5.5 ≤ M < 6.0	615	54
6.0 ≤ M < 6.5	790	61
6.5 ≤ M	915	70

Magnitude of an aftershock is less or equal to the magnitude of main shock. If an event occurs within time-space window of an aftershock of some main shock, but outside the time-space window of that main shock, then the event is not considered as an aftershock, unless it is formally the direct aftershock of another main shock.

Step 3. Identification of chains

A chain captures a rise of earthquakes' correlation range in its vicinity. The earthquake chain is a cluster of epicenters formed by "neighbors" and extending over large distances (an order larger than the length of the future strong earthquake). Neighbors are statistically rare pairs of epicenters close in space and time.

The R-vicinity of a chain is defined as the smoothed envelope of the circles of a radius R drawn around each epicenter in the chain. We use R-vicinity for the analysis of intermediate-term precursors; R-vicinity defines also the spatial area of predictions.

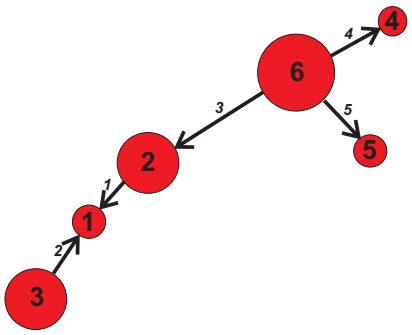

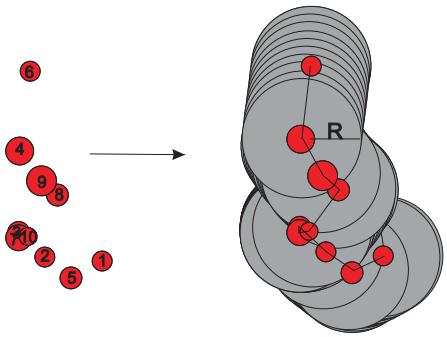

Neighbors: $Dr_{ij} <= r_0\ 10^{\,c\,\{\min(M_i,M_j)-2.5\}}$ and $Dt_{ij} <= t_0$

Time order is not taken into account

Step4. Pattern recognition

Each chain is only a candidate to be precursor with characteristic lead time months. To select precursory chains, intermediate-term seismicity precursory patterns (with characteristic lead time years) are analysed in the R-vicinity of each chain using pattern recognition algorithm "Hamming distance".

We consider 8 patterns representing four different types of precursors: rise of activity, rise of clustering, rise of the earthquake correlation range, transformation of Gutenberg-Richter relation [Keilis-Borok and Soloviev, 2003].

Step5. Estimation of the probability that the alarm is false. Prediction put on record.

The probability that the alarm-cabdidate will be a false alarm is estimated to the tested chain-candidate by the mean of numerous retrospective tests with variation of the learning set. We choose random subsets of the learning, and find threshold for functions. Then, we apply Hamming algorithm to the remaining part of the chains, and count the rate of false alarms using the number of precursors in the tested chain as the threshold. This rates give the estimation of the probability of false alarm.

We put prediction on record if this probability is estimated as less than 50%. Alarm duration is T_{al} starting time of last event in the precursory chain, area of alarm is R_{al}-vicinity of the chain. Retrospective analysis suggested T_{al} = 9 months, R_{al} = 50 km (100 km in North Pacific including Honshu-Hokkaido-S. Kurils).

This procedure helps not only to estimate the probability of false alarm, but also destroys a possible data over-fitting.

Step6. Estimation of the probability that a target earthquake will occure in time-space of alarm at random.

For the time-space of alarm we estimate the probability that strong earthquake occurs at random. We count the number of earthquakes with $M \geq M_0$ during the period available in the catalogue. If the number is too small (5 or less), we use extrapolation of the cumulated magnitude-frequency graph based on the interval (M_0-0.5, M_0). The obtained number is then converted to the frequency per interval of the alarm duration. This frequency serves as the sought value.

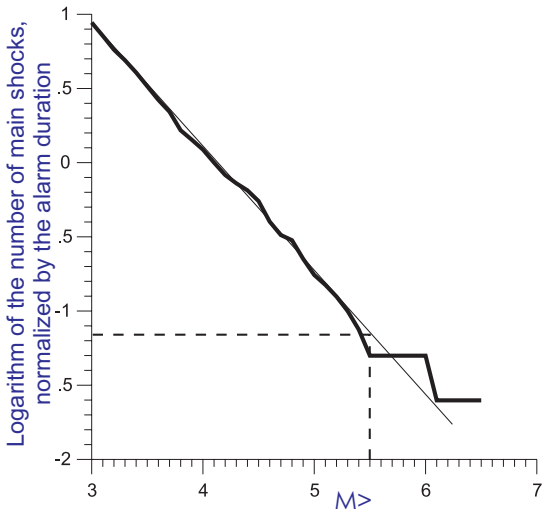

Step7. Prolongation and/or expansion of the alarm.

A precursory chain, once identified, may keep growing. We expand the time and space of the alarm only in case the spatial boundary of the alarm is shifted to more than 20 km or if necessary prolongation is 15 days or more. In that case the probability of false alarm is estimated anew; the alarm is updated if this estimate still is less than 50%. In the latter case the probability of a random occurrence of a target earthquake is re-estimated according to the new integral time-space of alarm.

Step8. Counting successes and failures.

If a target earthquake occurs within time-space area of an alarm, this is successful prediction. The alarm is not called off until it expires. If no target earthquakes occur within time-space area of an alarm, the alarm is false. If an earthquake occurs in the region considered, but not in a space-time area of alarm, this is a failure to predict.

Aftershocks are not targets of RTP predictions.

Results of the prospective test of RTP

Experiment in month-in-advance earthquake prediction by RTP algorithm

http://www.igpp.ucla.edu/prediction/rtp/

California and Western Nevada, M_{ANSS}>=6.4

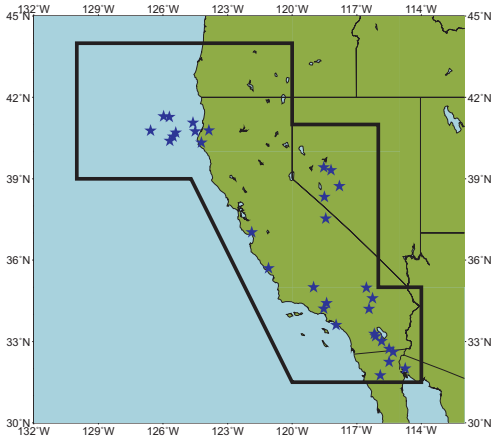

Honshu-Hokkaido-Southern Kuril, M_W>=7.2

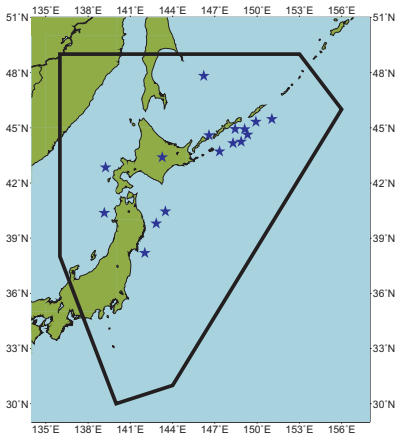

Eastern Mediterranean, M_W>=6.0

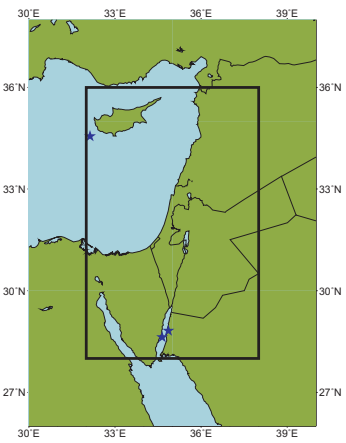

Central Apennines, Alps, Northern Dinarides and Po Valley, M>=5.5

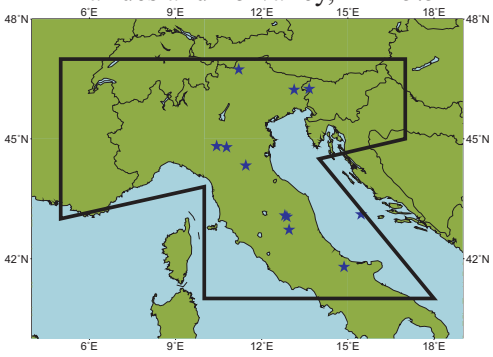

North Pacific, M_W>=7.2; experiment started from November 10, 2006

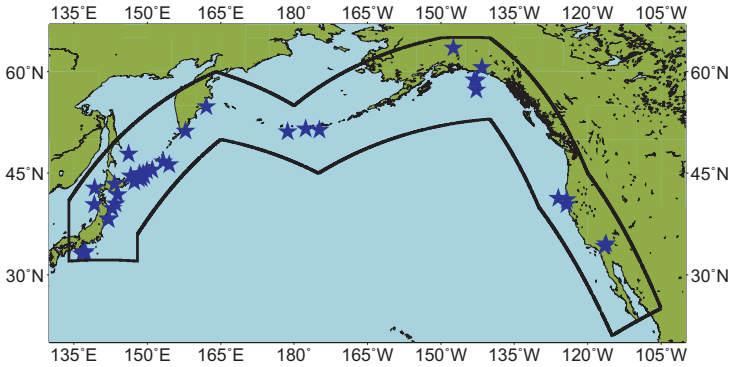

Regions covered by prediction

Advance prediction of Tokachi-oki earthquake, Japan, Sept. 25, 2003, M = 8.3

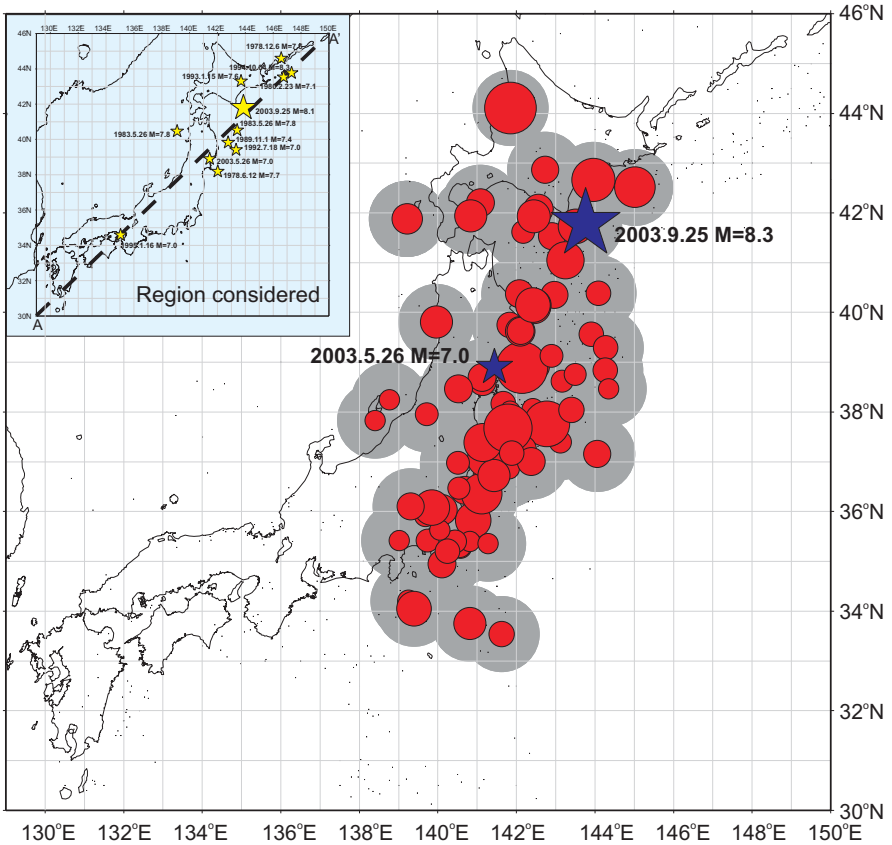

Dots show earthquakes, forming precursory chain. Stars - target earthquakes.

Case history, 2003

March 27: *Precursory chain* of earthquakes was formed. It indicates that an earthquake with magnitude 7 or more will occur in gray area within 9 months.

May 26: *Earthquake with magnitude 7.0* occurred in gray area; precursor was not reported in advance.

July 2: *Precursor reported* at IUGG (Sapporo, Japan).

Sept. 25: *Tokachi-oki earthquake* in gray area.

Advance short-term prediction of San Simeon earthquake in central California, M=6.5

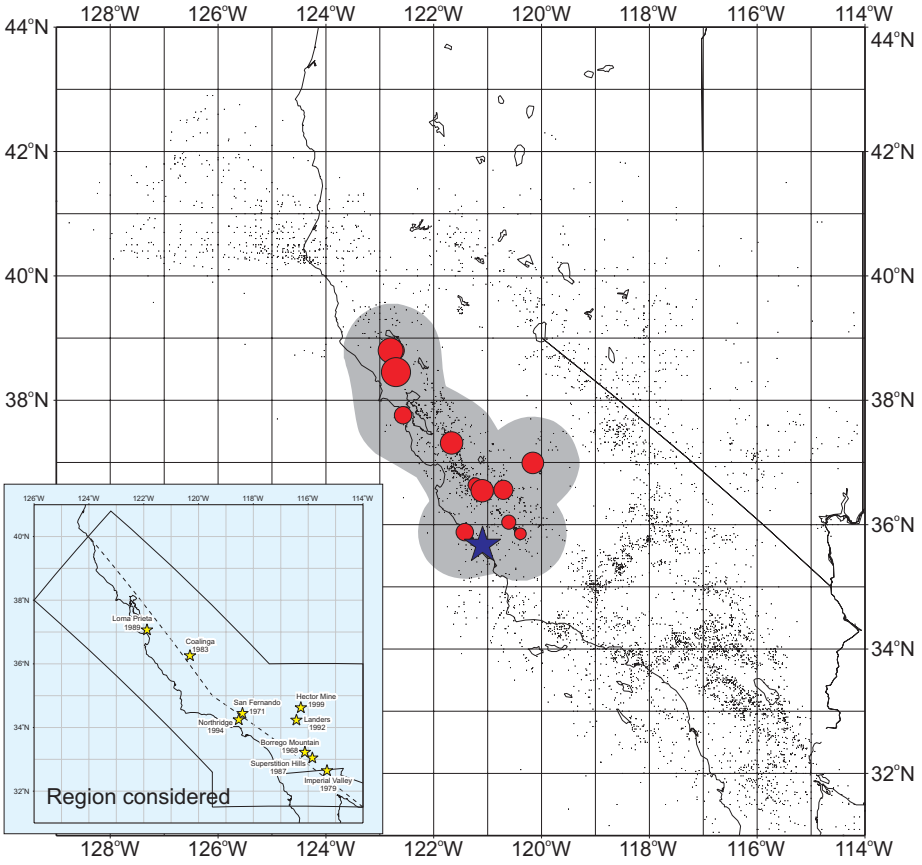

Case history, 2003
May 5: *Precursory chain* of earthquakes was formed. It indicates that an earthquake with magnitude 6.4 or more will occur in gray area within 9 months.
June 21: *Prediction was distributed* among relevant scientists and administrators.
Dec. 22: *San Simeon earthquake* (star).

Advance prediction of Simushir earthquake, Kuril islands, Russia, Nov. 15, 2006, M_w = 8.3 and second large earthquake, Jan. 13, 2007, M_w = 8.2

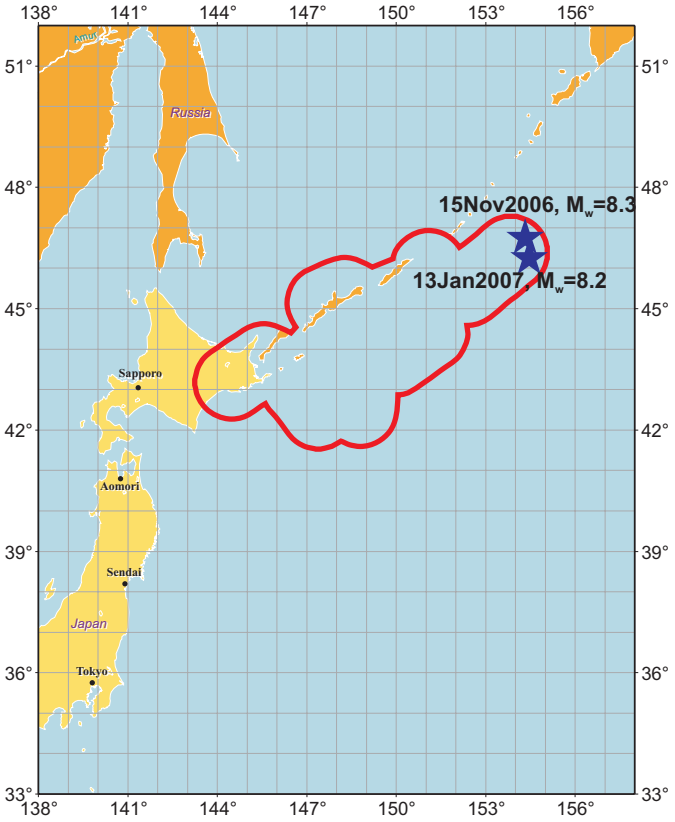

Case history, 2006-2007
Septemer 30, 2006: *Precursory chain* of earthquakes was formed. It indicates that an earthquake with magnitude 7.2 or more will occur in an area shown by red contour within 9 months.
October 9, 2006: *Precursor is reported* on the RTP web site (http://www.igpp.ucla.edu/prediction/rtp2/RTP10a.pdf)
Nov. 15, 2006 and Jan. 13, 2007: *Simushir earthquake,* M_W=8.3, and a second strong earthquake, M_W=8.2, have occured, their epicenters in the area shown by blue stars.

Advance prediction of Andreanof Islands earthquake, Aleutians, USA, Dec. 19, 2007, M_w = 7.2 using Reverse Tracing of Precursors (RTP)

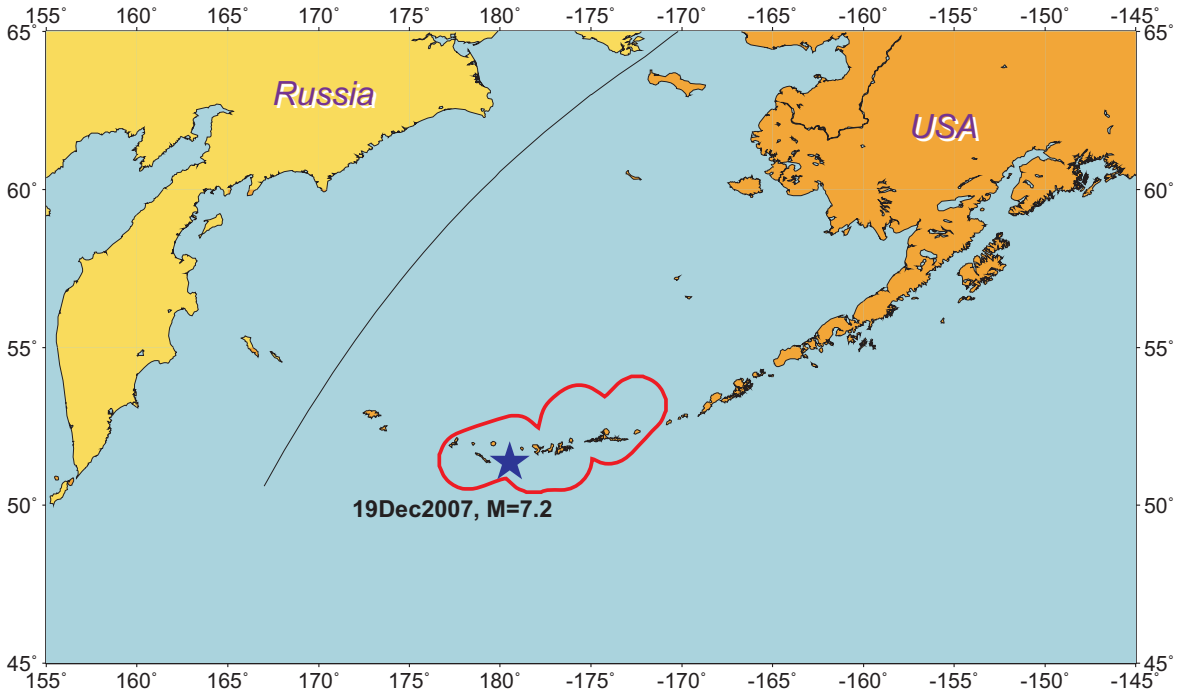

Case history, 2007

April 28: *Precursory chain* of earthquakes was formed. It indicates that an earthquake with magnitude 7.2 or more will occur in an area shown by red contour within 9 months.

July 28: *Precursor is reported* on the RTP web site (http://www.igpp.ucla.edu/prediction/rtp2/RTP_NP1a.pdf); an earthquake with magnitude M_W >= 7.2 is predicted to occur by January 28, 2008 in the area shown by red contour.

#	*Region/ target earthquakes*	*Period of alarm*	*Prediction was put on record on*	*Target or near target earthquake*	*Prediction outcome*	*Probability of a success by chance*
1	Japan M_{JMA}>=7.0	Mar 27, 2003 - - Jan 27, 2004	July 1, 2003	**Sep 25, 2003, M_w=8.3** ***within the alarm***	**Correct**	0.32
2	California M_{ANSS}>=6.4	May 5, 2003 - - Feb 27, 2004	June 24, 2003	**Dec 22, 2003, M=6.5** ***within the alarm***	**Correct**	0.01
3	Southern California M_{ANSS}>=6.4	Oct 29, 2003 - - Sep 05, 2004	May 12, 2004		**False alarm**	0.08
4	Honsu, Japan M_w>=7.2	Feb 8, 2004 - - Nov 8, 2004	June 1, 2004	**Sep 5, 2004, M_w=7.4** ***outside the region; 127 km outside alarm***	**False alarm**	0.03
5	Northern Dinarides M_w>=5.5	Feb 29, 2004 - - Nov 29, 2004	May 12, 2004	**Jul 12, 2004, M_w=5.2, M_L=5.7** ***within the alarm***	**False alarm**	0.03
6, 6a 6b 6c 6d 6e	Southern California M_{ANSS}>=6.4	Nov 14, 2004 - - Aug 14, 2005 - March 17, 2006 - Dec 24, 2006 - May 2, 2007 - Jan 28, 2008	Nov 16, 2004, Oct 5, 2005 Mar 17, 2006 Mar 30, 2006 Dec 24, 2006 May 2, 2007		**False alarm** **4.5 x 9 months**	0.28
7	Oregon off coast M_{ANSS}>=6.4	Nov 16, 2004 - - Aug 16, 2005	Jan 29, 2005	**Jun 15, 2005, M_w=7.2** ***60 km outside alarm***	**False alarm**	0.01
8, 8a	Central Italy M>=5.5	Jan 1, 2005 - Oct 1, 2005 - Feb 6, 2006	Jan 29, 2005, Oct 1, 2005		**False alarm** **1.5 x 9 months**	0.14
9	Honsu, Japan M_w>=7.2	June 14, 2005 - - Mar 14, 2006	Oct 1, 2005	**Aug 16, 2005, M_w=7.2** ***within the alarm***	**Correct** (*)	0.03
10, 10a	Hokkaido-S. Kurils M_w>=7.2	May 11, 2006 - - Feb 11, 2007 - June 30, 2007	May 22, 2006 Oct 9, 2006	**Nov 15, 2006 M_w=8.3** ***within the alarm***	**Correct** **1.5 x 9 months**	0.14
11	Italy, M>=5.5	May 2, 2006 - - Feb 3, 2007	June 12, 2006		**False alarm**	0.12
12	Oregon off coast M_{ANSS}>=6.4	Sept 23, 2006 - - June 23, 2007	Nov 10, 2006		**False alarm**	0.01
NP1, NP1a	Aleutians M_w>=7.2	Oct 28, 2006 - -July 28, 2007 - Jan 28, 2008	Nov 10, 2006 July 28, 2007	**Dec 19, 2007 M_w=7.2** ***within the alarm***	**Correct** **1.7 x 9 months**	0.04
14, 14a	Central California M_{ANSS}>=6.4	Jan 17, 2007 - - Oct 17, 2007 - Jan 14, 2008	Feb 1, 2007 Oct 31, 2007		**False alarm** **1.3 x 9 months**	0.03
NP2	Oregon off coast M_{ANSS}>=7.2	Aug 24, 2007 - May 24, 2008	Jan 5, 2008		**False alarm**	0.01
16	Oregon off coast M_{ANSS}>=6.4	Apr 14, 2008 - Jan 14, 2009	Apr 22, 2008		**False alarm**	0.01
17	Italy, M>=5.5	Apr 7, 2008 - Jan 7, 2009	Dec 23, 2008	**Dec 23, 2008, M=5.4** ***within the alarm***	**False alarm**	0.02
NP3	Oregon off coast M_{ANSS}>=6.4	Jul 17, 2008 - Apr 17, 2009	Jul 18, 2008		**False alarm**	0

Large earthquakes during the experiment

25-Sep-03	Japan	M_{JMA}= 8.0	**predicted**
22-Dec-03	Central CA	M=6.5	**predicted**
12-Jul-04	N. Dinarides	M_W=5.2	not a target: small magnitude (**near miss**, M_L = 5.7)
5-Sep-04	Japan	M_W = 7.4	not a target: outside region; (**near miss**, 140 km outside alarm)
15-Jun-05	CA Offshore	M_W = 7.2	**failure to predict** (near miss, 60 km outside alarm)
17-Jun-05	CA Offshore	M_W = 6.6	not a target: aftershock (outside prediction)
16-Aug-05	sea near Japan	M_W = 7.2	**predicted** (due to technical delay of data, the alarm was determined after the earthquake)
15-Nov-06	Kuriles	M_W = 8.3	**predicted**
13-Jan-07	Kuriles	M_W = 8.1	not a target: aftershock (within prediction)
19-Dec-07	Aleutians	M_W = 7.2	**predicted**
23-Dec-08	Italy	M=5.4	not a target: small magnitude
15-Jan-09	Kurils	M_W = 7.4	not a target: aftershock of the event of 13.01.07 (no alarm)
06-Apr-09	Central Italy	M=6.3	**failure to predict**

Integral statistics, September 2009

	Expected rate of targets in alarms k	Predicted n	Number of alarms	Expected rate of targets in regions K	Occurred N	τ=k/K	τ+η	probability gain n/k/(N/K)
California	0.41	1	7	2.58	2	0.16	0.66	3.13
Honshu to Kurils	0.45	3	4	3.00	3	0.15	0.18	6.67
Italy+	0.26	0	4	1.76	1	0.15	1.15	
E. Mediterranean	0	0	0	0.59	0	0	0	
N. Pacific (without Honshu to Kurils)	0.040	1	3	0.31	1	0.13	0.13	7.69
total	**1.16**	**5**	**18**	**8.24**	**7**	**0.14**	**0.49**	**5.10**

Available online at www.sciencedirect.com
SCIENCE DIRECT
Tectonophysics 413 (2006) 63–75
TECTONOPHYSICS
www.elsevier.com/locate/tecto

Short-term earthquake prediction by reverse analysis of lithosphere dynamics

P. Shebalin [a,d], V. Keilis-Borok [a,b,c,*], A. Gabrielov [e], I. Zaliapin [a,b], D. Turcotte [f]

[a] International Institute for Earthquake Prediction Theory and Mathematical Geophysics, Russian Ac. Sci., Warshavskoe sh., 79, korp. 2, Moscow, 113556, Russia
[b] Institute of Geophysics and Planetary Physics, University of California, Los Angeles, CA 90095-1567, USA
[c] Department of Earth and Space Sciences, University of California, Los Angeles, CA 90095-1567, USA
[d] Institut de Physique du Globe de Paris, 4 Place Jussieu, 75252, Paris Cedex 05, France
[e] Departments of Mathematics and Earth and Atmospheric Sciences, Purdue University, West Lafayette, IN 47907-1395, USA
[f] Department of Geology, University of California, Davis, CA 95616, USA

Received 24 December 2004; received in revised form 14 June 2005; accepted 4 October 2005
Available online 13 December 2005

Abstract

Short-term earthquake prediction, months in advance, is an elusive goal of earth sciences, of great importance for fundamental science and for disaster preparedness. Here, we describe a methodology for short-term prediction named RTP (Reverse Tracing of Precursors). Using this methodology the San Simeon earthquake in Central California (magnitude 6.5, Dec. 22, 2003) and the Tokachi-Oki earthquake in Northern Japan (magnitude 8.1, Sept. 25, 2003) were predicted 6 and 7 months in advance, respectively. The physical basis of RTP can be summed up as follows: An earthquake is generated by two interacting processes in a fault network: an accumulation of energy that the earthquake will release and a rise of instability triggering this release. Energy is carried by the stress field, instability is carried by the difference between the stress and strength fields. Both processes can be detected and characterized by "premonitory" patterns of seismicity or other relevant fields. Here, we consider an ensemble of premonitory seismicity patterns. RTP methodology is able to reconstruct these patterns by tracing their sequence backwards in time. The principles of RTP are not specific to earthquakes and may be applicable to critical transitions in a wide class of hierarchical non-linear systems.

Keywords: Reverse tracing of precursors; Short-term earthquake prediction

1. Introduction

There is increasing evidence that variations in regional seismicity occur prior to intermediate and large earthquakes (Keilis-Borok et al., 1980; Mogi, 1981; Caputo et al., 1983; Sykes, 1983; Keilis-Borok, 1990; Ma et al., 1990; Molchan et al., 1990; Knopoff et al., 1996; Bowman et al., 1998). Using pattern recognition techniques a series of algorithms have been developed which provide intermediate-term and long-term predictions with lead times of years to decades respectively (Keilis-Borok and Shebalin, 1999; Keilis-Borok, 2002; Keilis-Borok and Soloviev, 2003; Rundle et al., 2003). In this paper an algorithm is introduced that has successfully made short-term earthquake predictions, i.e.

* Corresponding author. Institute of Geophysics and Planetary Physics, University of California, Los Angeles, CA 90095-1567, USA.
E-mail address: vkb@ess.ucla.edu (V. Keilis-Borok).

0040-1951/$ - see front matter © 2005 Elsevier B.V. All rights reserved.
doi:10.1016/j.tecto.2005.10.033

months in advance (Shebalin et al., 2004; Keilis-Borok et al., 2004). This algorithm is currently tested by advance prediction in several seismically active regions and its performance is yet to be validated. However, the first successes along with the novelty of the methodology used in this algorithm and a multitude of its possible applications motivate us to describe here its underlying ideas and techniques.

It should be emphasized that there are two quite different approaches to earthquake prediction. The first is to make continuous predictions; in terms of earthquakes, this requires the specification of earthquake risk at all spatial points at each time instant. This approach is very useful when predicting a large number of small to intermediate earthquake since one can directly compare the observed and predicted seismic rates (probabilities, intensities, etc.) using the log-likelihood paradigm (Daley and Vere-Jones, 2004) or the least-square discrepancy (Whittle, 1963). The second approach that is used here is binary: an earthquake is forecast (predicted) for a specified area and time window, called *alarm region* or *alarm*. This approach is better justified when predicting extremely rare large events, so the direct comparison of the predicted continuous rate with a couple of observed earthquakes is rather problematic (Molchan, 1990, 2003). Our goal is to narrow down the area and time duration of alarms, within which a target earthquake is expected. Prediction is targeted at the large and therefore rare earthquakes; in a typical alarm area they occur on average once in 10–20 years. Our prediction should capture the target within an interval 20–30 times smaller, since a short-term alarm lasts months. Thus our alarms should be equally rare and each correct alarm would typically capture only one target.

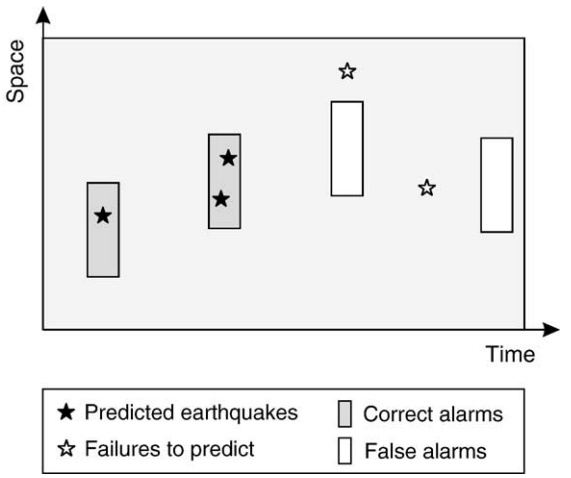

Fig. 1. Possible outcomes of prediction. For simplicity the territory where the prediction is made is represented by a 1D 'Space' axis. Rectangles—space–time areas covered by correct (gray) and false (white) alarms respectively.

An early theoretical discussion of the necessity of a binary approach instead of a continuous one in predicting rare point events is given in (Lindgren, 1975, 1985; De Mare, 1980). The difference between continuous and binary predictions has been widely recognized in weather forecasting (Jolliffe and Stephenson, 2003). An example of binary forecast is a tornado warning issued for a specified area and time window. Tornado warnings are analogous to the earthquake alarms considered in this paper. Possible outcomes of such predictions are illustrated in Fig. 1. In this scheme, we have two types of errors: failures to predict (target earthquake outside alarm region) and false alarms (no target earthquakes within an alarm); a prediction algorithm is also characterized by the total time–space covered by the alarms. Probability of errors of different types is estimated using a sequence of predictions and is visually represented in the error diagrams (Sect. 3 below; Molchan, 1990, 2003). An analogous approach in weather forecasting is the *relative operating characteristic* diagram (Jolliffe and Stephenson, 2003).

2. Reverse Tracing of Precursors (RTP)

We will now outline the RTP (Reverse Tracing of Precursors) approach to short-term earthquake forecasting. Technical details are given in the Appendix. Three aspects of RTP are important:

(i) *Precursory chains* that reflect the premonitory increase of the earthquakes' correlation range; qualitatively, these chains are the dense, long, and rapidly formed sequences of small and medium sized earthquakes. Their definition generalizes premonitory seismicity patterns ROC and ACCORD. Heuristically, the pattern ROC ensures the ongoing increase of earthquake correlation-range, expressed via the pair-wise correlation function; while ACCORD reflects simultaneous activation of several major parts of the regional fault network. They represent complimentary approaches to detecting the earthquake correlation. Formal definitions of these patterns as well as their performance in synthetic and observed seismicity can be found in (Gabrielov et al., 2000; Shebalin et al., 2000; Zaliapin et al., 2002, 2003; Keilis-Borok et al., 2002). An alternative approach to measuring the earthquake correlation was introduced in (Zöller and Hainzl, 2001; Zöller et al., 2001).

(ii) *Intermediate-term patterns*, originally found in the modeled and observed seismicity (Prozorov and Schreider, 1990; Keilis-Borok and Shebalin, 1999; Gabrielov et al., 2000; Keilis-Borok, 2002; Keilis-Borok and Soloviev, 2003; Zaliapin et al., 2003). They reflect four major types of premonitory phe-

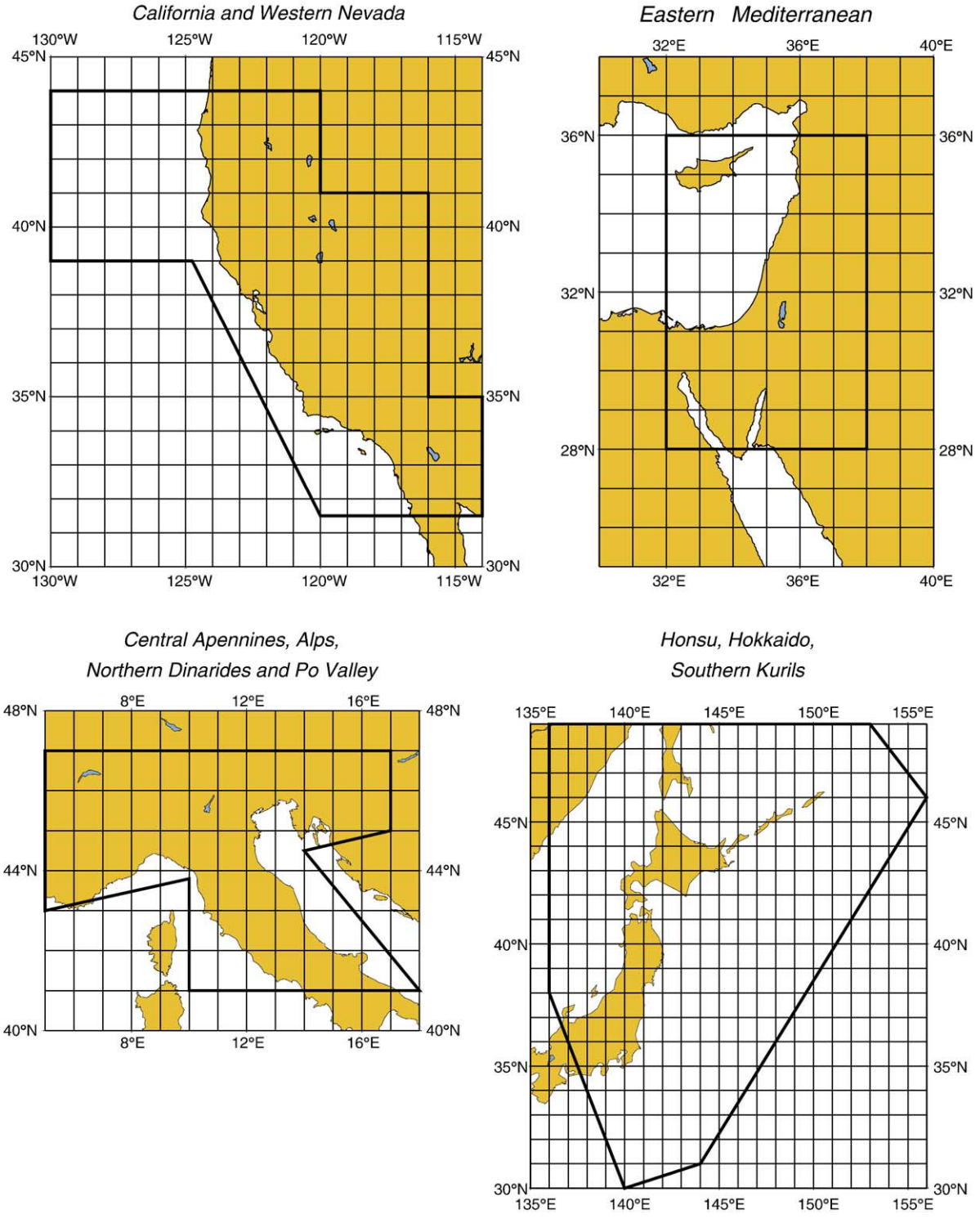

Fig. 2. Regions where the proposed algorithm was tested by advance prediction. See text for details.

nomena: rise of seismic activity, rise of earthquakes' clustering, rise of earthquakes correlation range, and a transformation of the magnitude–frequency (Gutenberg–Richter) relation towards an increasing share of relatively large magnitudes.

(iii) *Pattern recognition of infrequent events* is used to define the precursory combination of the patterns. Specifically, we used the Hamming algorithm which in our case is analogous to voting (Keilis-Borok and Soloviev, 2003); this algorithm is a standard tool in making a decision by considering several "opinions". Formally, the Hamming distance between two Boolean vectors of the same length is defined as the number of their non-coincident symbols. In our problem, the Hamming distance is the number of emergent intermediate-term premonitory patterns.

RTP analysis consists of the following stages. First, we detect chains—the "candidates" for the short-term precursors. We have found that precursory chains emerge within months before most of the target earthquakes. However, up to 90% of the chains are not followed so closely by strong earthquakes and in prediction they would cause false alarms. To eliminate false alarms, we next determine which intermediate-term precursors have occurred in the vicinity of each candidate within few years preceding it. Finally, we apply pattern recognition: knowing for each candidate what intermediate-term patterns have preceded it, we recognize which chains are precursory and which are false alarms. Specifically, we discriminate precursory and non-precursory chains using a set of M individual intermediate-term premonitory patterns. Some of them give premonitory signal (emerge) while other do not. The current state of the patterns is represented by a $M \times 1$ Boolean vector indicating which pattern emerge (1) and which is not (0). A zero vector would indicate that none of the patterns emerge and the chain is most probably not precursory, while a vector consisting of all ones that all the patterns emerge and the chain is most probably precursory. Hamming distance, defined as the number of ones in our Boolean vector, shows how far the vector is from a zero one; in other words, how many patterns "voted" for making the chain precursory. If sufficient number of votes is accumulated (the threshold is established during the learning) the chain is considered precursory. This brings us to the prediction proper. The emergence of each precursory chain starts an alarm: a target earthquake is expected during τ months after the chain was formed and in its formally defined vicinity.

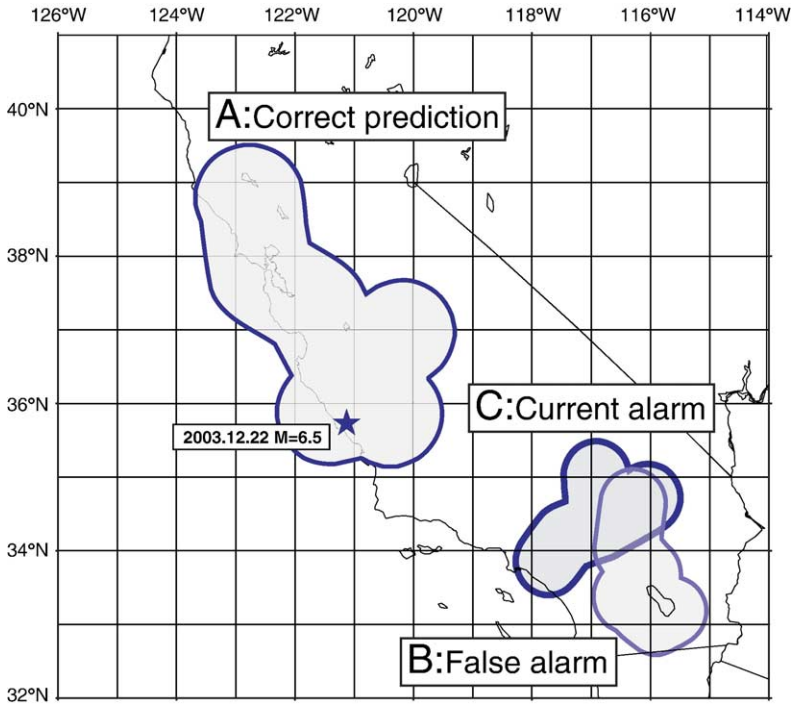

Fig. 3. Results of advance prediction in California. The advance prediction started in July 2003. Three alarms were issued: one correct (marked A), one false (B), one current (C).

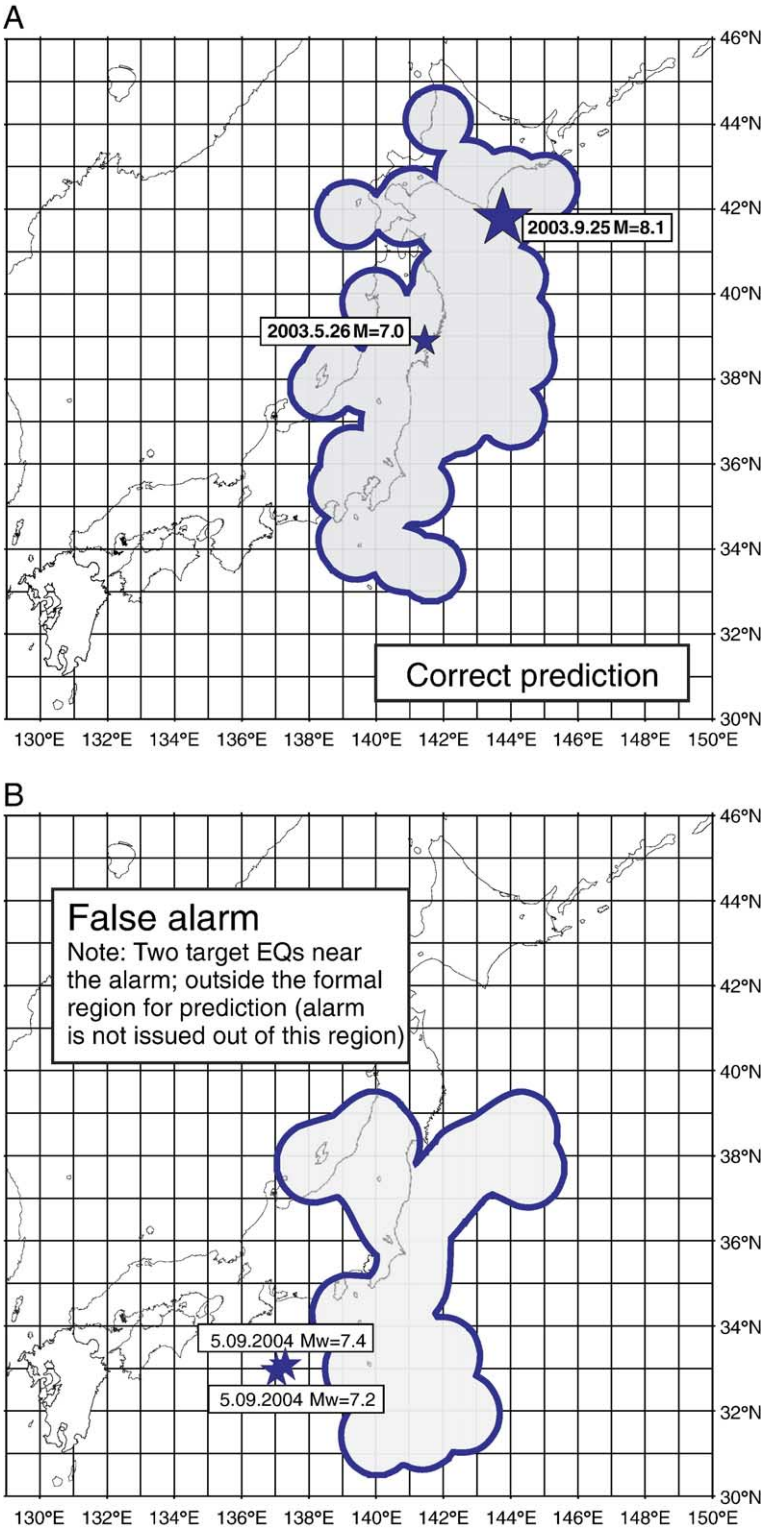

Fig. 4. Results of advance prediction in Japan. The advance prediction started in July 2003. Two alarms were issued: one correct (panel A), and one false (panel B). We notice that two target earthquakes occurred outside the formal prediction region near the boundaries of our false alarm; if one extended the prediction region to include these two target earthquakes, they would be successfully predicted with the current values of algorithm parameters.

Thus, the precursory chain indicates the narrow area of a possibly complex shape (the chain vicinity) where intermediate-term precursors should be looked for. Their presence in turn validates the chain, as a short-term precursor. A chain is considered first although it emerges later—hence our analysis is called *reverse*.

3. Performance

We have tested our algorithm by advance prediction in Southern and Central California using the earthquake catalog ANSS/CNSS starting from January 1965. First, the data for 1965–1994 have been used for "learning", i.e. self-adaptation of some of the parameters (see Appendix A3). Then, the resulting rule was tested on independent data (i.e. the data not used for learning) for the period from January 1995 to May 2003. In June 2003 we have launched advance prediction. The only target earthquake that happened in the prediction region during the advance phase of the experiment (the San Simeon earthquake, December 22, 2003, $M=6.5$) was successfully predicted. The alarm capturing this earthquake started on May 5, 2003—the date when the precursory chain triggering the alarm was completed. This alarm was reported on June 21 of the same year (Aki et al., 2003).

The algorithm has also been applied to the territories of Japan; Central Apennines, Alps, Northern Dinarides and Po valley; and Eastern Mediterranean (Figs. 2–5) with magnitude of target earthquakes $M\geq 7$, $M\geq 5.5$ and $M\geq 6.5$ respectively. In Japan, the learning was performed during 1975–2003, and advance prediction started on July 1, 2003 (Shebalin et al., 2003). In Central Apennines, Alps, Northern Dinarides and Po valley the learning was performed during 1970–1990, and advance prediction started on May 12, 2004. In Eastern Mediterranean the learning was performed during 1983–2003, and advance prediction started on May 12, 2004. The intermediate-term patterns (see Appendix A3) showed amazing self-adjustment: they were applicable within all three regions, and to all chains within each region, with the same values of their four numerical parameters.

The Tokachi-Oki, Japan, earthquake, 25 September 2003, $M=8.1$, has been also predicted in advance: the alarm started on 27 March, 2003 and was reported on 2 July 2003 (Shebalin et al., 2004).

During the time period covered by our advance prediction experiment, two target earthquakes have occurred; both of them have been predicted. Three false alarms were issued; one alarm is current. Figs. 3–5 and Table 1 summarize the results of the experiment. It is worth noticing for further research that a large earthquake ($M_L=5.7$, $M_W=5.3$) occurred within the alarm issued in Northern Dinarides; and that two target earthquakes ($M_W=7.4$, $M_W=7.2$) occurred near one of the alarms issued in Japan, but outside the formal prediction region. A retrospective analysis for an extended

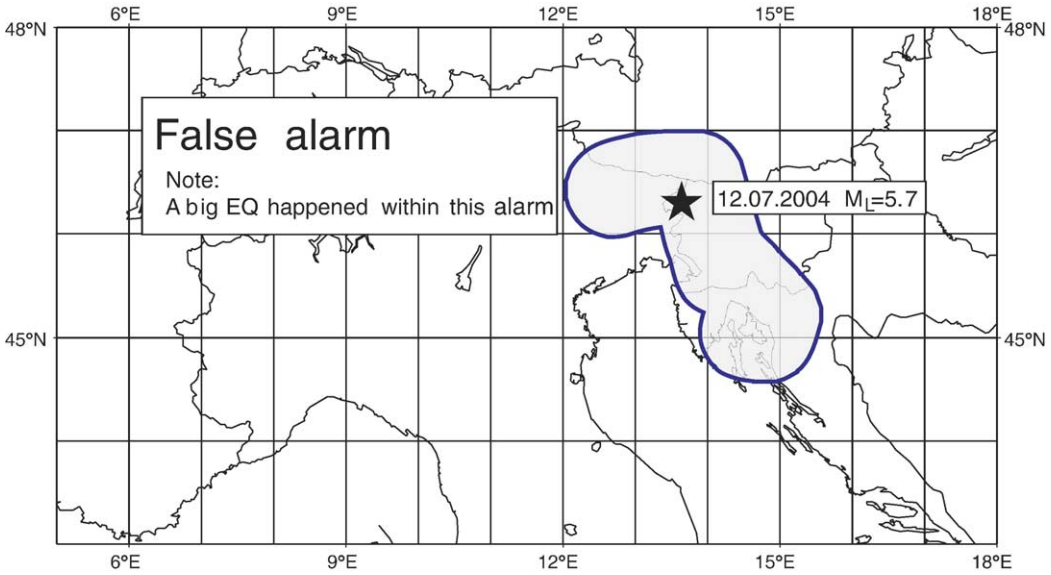

Fig. 5. Results of advance prediction in Northern Dinarides. The advance prediction started in May 2004. One false alarm was issued. We notice that a big earthquake happened within our false alarm; this earthquake formally does not fit the prediction as its magnitude $M_W=5.3$ (prediction was done for $M_W>=5.5$).

Table 1
Results of the advance prediction experiment

Region/target earthquakes	Alarm duration	Probability that a target earthquake will occur at random in the time–area of alarm[a]
Japan $M_{JMA} \geq 7.0$	27 Mar 2003–27 Jan 2004 Tokachi-Oki, 25 Sep 2003, $M_W = 8.3$	0.25
Central and Southern California $M_{ANSS} \geq 6.4$	5 May 2003–27 Feb 2004 San Simeon, 22 Dec 2004, $M = 6.5$	0.05
Southern California $M_{ANSS} \geq 6.4$	29 Oct 2003–05 Sep 2004 False alarm	0.08
Honsu, Japan $M_W \geq 7.2$	8 Feb 2004–8 Nov 2004 False alarm (note: two quakes, $M_W = 7.4$ and $M_W = 7.2$ outside formal region boundaries)	0.07
Northern Dinarides $M_W \geq 5.5$	29 Feb 2004–29 Nov 2004 False alarm (note: $M_W = 5.3$, $M_L = 5.7$ in the area of alarm)	0.07
Southern California $M_{ANSS} \geq 6.4$	14 Nov 2004–14 Aug 2005 Current alarm	0.05

[a] See Appendix A7 for the explanations of how this estimation was obtained.

region gives a successful prediction for those two earthquakes.

4. Prediction quality

As we mentioned in the Introduction, the problem of evaluating a binary prediction requires special tools.

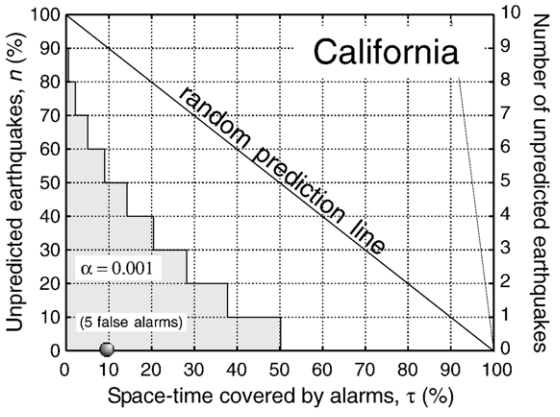

Fig. 6. Significance of prediction in California: an illustration (see Appendix A6 for details). Shaded ball shows performance of the prediction algorithm during the time interval considered. A perfect prediction would lie in the origin. Random binomial predictions (alarm is declared for each elementary spatio-temporal unit with a fixed probability τ) asymptotically occupy the diagonal, but might deviate from it with finite number of target earthquakes. Random predictions with fixed τ fall in the grey area with probability $\alpha = 0.001$. Note that the shape of the grey area depends on the number of the target earthquakes that actually happened within the prediction region.

The main difference from evaluating a continuous prediction is that we can no longer use a single measure of discrepancy between prediction and observations (one faces the same situation in classical hypothesis testing where errors of two types are introduced). We use three interdependent measures of prediction quality, defined in Appendix A5: fraction of unpredicted earthquakes, n; fraction of false alarms, f; and the space–time τ covered by all alarms together, normalized by the whole space–time considered. The space is measured not in km^2 but in long-term average of seismicity. Specifically, we used the average number of mainshocks with $m \geq 4$. The optimal tradeoff between different characteristics depends on a loss function $L(n,f,\tau)$ for preparedness measures (Molchan, 1990, 2003).

The *error diagram* juxtaposes the prediction errors; each particular prediction corresponds to a single point in (n, τ, f) space. The error diagram is used to evaluate the predictive power of our prediction algorithm and its stability. For illustration, the error diagram for our prediction experiment in California during 1964–2005 is shown in Fig. 6; it shows the relative alarm coverage τ (10%) vs. the number of failures to predict (0); the number of false alarms (5) is indicated in parentheses. A more detailed discussion of error diagram approach is given in Appendix A6.

5. Discussion

1. *A possible physical mechanism* underlying the RTP methodology is based on models of dynamical

systems (Gabrielov et al., 2000; Zaliapin et al., 2003) and geodynamical models (Rundquist and Soloviev, 1999). Precursory chains outline the areas where instability is accumulated months before a target earthquake. This instability reveals itself through an increase of the earthquake correlation range. Intermediate-term premonitory seismicity patterns considered reflect the accumulation of energy and instability necessary and sufficient to trigger an earthquake, in the area outlined by a precursory chain, but years before the chain. In more general terms, RTP identifies a small-scale perturbation that carries a memory of the larger scale history of a complex system (in our case, the fault network). Increases of the correlation range are a known symptom of critical transitions in statistical physics and of bifurcation in nonlinear dynamics (Kadanoff, 2000). Typically for premonitory patterns of this kind precursors considered are sporadic short-lived phenomena not necessarily reflecting the steady trends of seismicity. This suggests that both patterns are symptoms but not the causes of a target earthquake: they signal its approach but do not trigger it. Such sporadic precursors to critical phenomena have been found also in socio-economic complex systems (Keilis-Borok et al., 2000).

2. It seems promising to apply RTP analysis to the detection of earthquake precursors in the other relevant and available data such as electromagnetic fields (Uyeda and Park, 2002), fluid regime (Ma et al., 1990), InSAR and GPS (Simons et al., 2002). The first positive result has been obtained with precursors gauging interaction between the ductile and brittle layers of the Earth crust; this opens a highly promising link of geodynamics and nonlinear dynamics approaches to prediction (Jin et al., 2004).

3. *The methodological advantage* of RTP over a direct analysis is in the drastic reduction in dimensionality of the parameter space where premonitory patterns are looked for. We have found here the patterns formed in narrow areas different from case to case, whose shape might be complicated, and with diverse size. To find these areas by a trial-and-error procedure would require trying different shapes, sizes, and locations, which is hardly realistic. Reverse analysis resolves this impasse, determining from the start a limited number of the areas to consider. Thus, RTP analysis provides a common methodological approach to the prediction of avalanches in a wide class of the complex systems, formed separately or jointly by nature and society.

4. The only decisive test of any prediction theory is an experiment in advance prediction. Such an experiment for the methodology described above was launched in June 2003 and is currently maintained by University of California Los Angeles (USA), Russian Academy of Sciences, and Institut de Physique du Globe de Paris (France). The complete results will be published elsewhere. The goal of this paper is to present the essential underlying concepts and report its first successes to a broad range of multidisciplinary experts, attracting their attention to the possibility of exploring premonitory patterns in diverse physical fields using the RTP methodology.

Acknowledgements

We are grateful to K. Aki, M. Ghil, A. Jin, L. Knopoff, J. McWilliams, and A. Soloviev for tough constructive criticism; to A. Kashina for inspired editing; and to D. Shatto for help in preparing the manuscript. This study was supported by the 21st Century Collaborative Activity Award for Studying Complex Systems from the James S. McDonnell Foundation, the National Science Foundation under grant ATM 0327558, and ISTC project 1538. The earthquake catalogs are compiled by Advanced National Seismic System (ANSS), Geophysical Institute of Israel (GII), and Japanese Meteorological Agency (JMA). The JMA catalog was received through the Japan Meteorological Business Support Center.

Appendix A

A.1. Earthquake catalogs

The data used in analysis are provided by the routinely compiled earthquake catalogs, which present at the moment the most accurate and complete information about the dynamics of seismicity. The earthquake catalog is taken from ANSS/CNSS (ANSS/CNSS Worldwide Earthquake Catalog, 1965–2003) and NEIC. We use a common representation of the earthquake catalog $\{t_j,\ \varphi_j,\ \lambda_j,\ M_j,\ b_j\}$, $j=1, 2, \ldots$ Here t_j is the time of an earthquake, $t_j \geq t_{j-1}$; φ_j and λ_j—latitude and longitude of its epicenter; and M_j magnitude. We consider the earthquakes with magnitude $M \geq M_{\min}$. As in most premonitory patterns of that family (Keilis-Borok, 2002) aftershocks are eliminated from the catalog; however, an integral measure of aftershocks activity b_j is retained for each remaining earthquake (main shocks and foreshocks); b_j is the number of aftershocks occurring immediately after an earthquake (e.g. within 2 days).

A.2. Chains

A chain captures a rise of earthquakes' correlation range in its vicinity. Let us call two earthquakes "neighbors" if their epicenters are closer than r and their times are closer than τ_0. A chain is a sequence of earthquakes where each earthquake has at least one neighbor belonging to that sequence and, therefore, no neighbors outside the sequence. he average density of epicenters decreases with increasing magnitudes. Accordingly, r is normalized as $r=r_0 10^{c(m-2.5)}$, where m is the smallest magnitude in the pair. The R-vicinity of a chain is outlined by the smoothed envelope of the circles of a radius R drawn around each epicenter in the chain. We consider only the chains with two sufficiently large characteristics: number of earthquakes $k \geq k_0$, maximal distance between epicenters $l \geq l_0$. Two parameters of the chains are common for all the regions: $r_0=50$ km, $c=0.35$. Other parameters are common for all chains within a region, but differ between regions as follows: Southern California, $\tau_0=20$ days, $k_0=6$, $M_{\min}=2.9$, $l_0=175$ km; Central California, $\tau_0=30$ days, $k_0=10$, $M_{\min}=2.9$, $l_0=250$ km; in Japan, $\tau_0=20$ days, $k_0=10$, $M_{\min}=3.6$, $l_0=350$ km, $\gamma_0=0.4$; Eastern Mediterranean, $\tau_0=40$ days, $k_0=6$, $M_{\min}=3.0$, $l_0=200$ km.

A.3. Intermediate-term patterns

We look for intermediate-term patterns in the R-vicinity of each chain within T years preceding it. To detect a pattern P we compute a function $F_P(t_j)$ defined in the "event window" (Keilis-Borok and Soloviev, 2003), i.e. on the sequence of N consecutive earthquakes with indexes $j-N+1$, $j-N+2,\ldots$, j. In R-vicinity of each chain we normalize seismicity by the lower magnitude cutoff M^*. The latter is derived from magnitude–frequency relation, by the condition $n(M^*)=n^*$; here $n(M^*)$ is the annual number of earthquakes with magnitude $M \geq M^*$.

Four functions represent *a rise of activity*. Namely

$$\text{"Activity"}\ F_U(t_j) = \frac{N}{t_j - t_{j-N+1}} \tag{A1}$$

is inversely proportional to the time it took to accumulate the most recent N earthquakes;

$$\text{"Sigma"}\ F_\Sigma(t_j) = \sum_{k=j-N+1}^{j} 10^{M_k - M^*} \tag{A2}$$

is shown to be a crude measure of total area of fault-breaks during the most recent N earthquakes (Keilis-Borok, 2002);

$$\text{"Rise of magnitudes"}, F_M(t_j) = \frac{2}{[N/2]}\left(\sum_{k=j-N+1}^{j-N+[N/2]} M_k - \sum_{k=j-[N/2]+1}^{j} M_k\right) \tag{A3}$$

is the difference between the average magnitude of the last $[N/2]$ earthquakes and that of the first $[N/2]$ earthquakes within a series of N;

$$\text{"Acceleration"}\ F_C(t_j) = \frac{1}{[N/2]}\left(\sum_{k=j-N+1}^{j-N+[N/2]} \frac{1}{t_k t_{k-1}} - \sum_{k=j-[N/2]+1}^{j} \frac{1}{t_k - t_{k-1}}\right) \tag{A4}$$

is connected to the function "Activity". "Acceleration" increases if intercurrence time between earthquakes decreases with time.

Here $[x]$ denotes integer part of x.

Two functions depict *a rise of clustering*. The first one, "Swarm", reflects clustering of mainshocks:

$$F_W(t_j) = 1 - \frac{A_r(t_j)}{\pi r^2 N}. \tag{A5}$$

Here A_r is the area of the union of circles of radius r centered at N epicenters in the sequence. The second one, "b-micro", reflects clustering of aftershocks:

$$F_{b_\mu}(t_j) = \sum_{k=j-N+1}^{j} \sum_{l} 10^{M_{kl} - M^*}. \tag{A6}$$

Here M_{kl}, $l=1, 2,\ldots$ are the magnitudes of the aftershocks of the kth main shock within the first 2 days after the main shock.

The *rise of earthquakes correlation range* is depicted by function

$$\text{"Accord"}\ F_A(t_j) = \frac{A_r(t_j)}{\pi r^2}, \tag{A7}$$

which increases if earthquakes are widely distributed in space and their r-neighbourhoods are barely overlapping. Finally, *the transformation of Gutenberg–Richter relation* is reflected by function

$$\text{"Gamma"}\ F_\gamma(t_j) = \frac{1}{N_{M_k \geq M_{1/2}}} \sum_{M_k \geq M_{1/2}} \left(M_k - M^*\right), \tag{A8}$$

which increases if the magnitude distribution is shifted to the larger magnitudes (e.g. if the GR slope is decreasing). Here $M_{1/2}$ is the median of magnitudes of N earthquakes in our sequence.

Altogether the eight functions are determined by five parameters. In each region we used the same eight combinations of these parameters: $n^*=10$ and $R=50$ km or $n^*=20$ and $R=100$ km, $N=10$ or 50, $T=6$ or 24 months, $r=50$ km. Emergence of a pattern at the moment t is captured by the condition $F_P(t)\geq C_P$. Each threshold C_P is determined automatically at the learning stage. It minimises the sum $n+f$; here n is the rate of failures to predict and f is the rate of false alarms in prediction with a single pattern P.

In predicting the San Simeon and Tokachi-Oki earthquakes we used $R=75$ km to define the R-vicinity of a chain. This choice corresponds to the average of $R=50$ km and $R=100$ km used in our definition of the intermediate-term patterns. In the ongoing experiment we use $R=100$ km in Japan (region with the highest magnitude of a target earthquake, $M_W=7.2$) and $R=50$ km in all other regions.

A.4. Prediction

Final stage is recognition of precursory chain and issuing an alarm: A chain is recognised as precursory if it was preceded by C or more intermediate-term patterns out of the ensemble considered. The threshold C controls the trade-off between the rates of false alarms and failures to predict. Emergence of precursory chain triggers an alarm in its R-vicinity for the Δ months; statistics of past alarms suggests $\Delta=9$ months. A precursory chain may keep growing accumulating subsequent earthquakes. In that case the alarm is extended. If a target earthquake occurs in the R-vicinity of a chain, then the chain no longer grows, but the alarm (if it has been diagnosed for that chain) is not called off. After a target earthquake all other chains containing its epicenter within the R-vicinity are disregarded during the period Δ.

A.5. Quality of prediction

Suppose that the prediction was performed during the time interval of length T (year) within the region Ω with the area S (km^2); N large earthquakes occurred within this period; A alarms were declared and A_f of them were false; all the alarms together covered the spatio-temporal volume V_A (year$\times$km^2); N_f target earthquakes were unpredicted. Prediction is described by the following dimensionless errors: the fraction of unpredicted earthquakes, $n=N_f/N$; the relative alarm coverage, $\tau=V_A/(T\times S)$; the fraction of false alarms, $f=A_f/A$.

When calculating the alarm coverage, it might be advantageous to take into account the observed inhomogeneities of the earthquake spatial distribution. In our prediction experiment, the relative alarm coverage for an alarm that spans the time T_A and space S_A is calculated as

$$\tau_A = \frac{T_A}{T}\frac{\int_{S_A} \mathrm{d}N_4(r)}{\int_S dN_4(r)} = \frac{T_A}{T}\frac{\#\{\text{EQ with } m\geq 4 \text{ within } S_A\}}{\#\{\text{EQ with } m\geq 4 \text{ within } S\}}. \quad (A9)$$

Here by $N_4(r)$ we denote the 2D point process of earthquakes with magnitude $m\geq 4$. The total alarm coverage is the sum of that for all individual alarms.

A.6. Significance level: random binomial prediction

To evaluate significance of a prediction one typically evaluates the chances of getting the same or better result (same or smaller values of errors) when there is no dependence between alarms and the occurrence of target earthquakes. An extremely simple but easily tractable model of prediction which produces alarms independent of the target earthquakes is *random binomial prediction* (Molchan, 2003): One divides the space–time considered for prediction into M small equal bins and declares alarm in each of them with fixed probability p. Indeed, this approach is highly unrealistic. Nevertheless, considered as a null (random) prediction model, it provides a good coarse estimation of the algorithm predictive power. Significance with respect to a random binomial prediction may serve as a necessary, but not sufficient, condition for validating an algorithm.

It is readily checked that expected values of alarm coverage τ and fraction f of failures to predict in the binomial prediction are given by:

$$E(\tau)=p, \qquad E(f)=1-p$$

so the point corresponding to this prediction is on the diagonal $f=(1-\tau)$ in the 2D (τ,f)-section of the error diagram. The probability to predict exactly $N-N_f$ out of N target earthquakes, assuming that no more than one target earthquake may occur within a single bin, is given by binomial distribution

$$\Pr\{\text{predict } N-N_f \text{ out of } N\} = \binom{N}{N_f} p^{N-N_f}(1-p)^{N_f}. \quad (A10)$$

The probability to predict $N-N_f$ out of N target earthquakes issuing alarm within k bins out of M is given by hypergeometric distribution

$$\Pr\{\text{predict } N-N_f \text{ out of } N \text{ declaring alarm in } k \text{ bins out of } M\} = \frac{\binom{k}{N-N_f}\binom{M-k}{N_f}}{\binom{M}{N}}. \quad \text{(A11)}$$

The number of false alarms can also be obtained, but because of the simplistic binomial rules, the number of binomial alarms (and false alarms) will be significantly larger than that in any realistic prediction (where alarm is typically declared for considerable spatio-temporal area, not for a small bin). Thus here we do not make any inference about false alarms using the binomial prediction model.

Using the above probabilities (A10, A11) one can construct different significance measures for a given prediction with errors (τ^*, n^*). One approach is to use the 2D (τ, n) distribution under the binomial model using (A10) with $p=\tau^*$, and evaluate probability of obtaining a prediction of the same or better quality, say

$$\Pr\{(\tau,n):\tau+n\le\tau^*+n^*\} \text{ or } Pr\{(\tau,n);\tau\le\tau^*\,\&\,n\le n^*\}.$$

Another approach is to use (A11) to find the probability to predict the same or larger number of earthquakes with the same total duration of alarms. The difference between using (A10) and (A11) is that in the first case we assume fixed *probability* of declaring an alarm, while in the second—fixed *duration* of alarm. Indeed, in generic cases both approaches give very similar evaluation of prediction performance.

To illustrate the above approach, Fig. 6 shows the error diagram for the results of our prediction experiment in California. Shaded ball represents the errors of our prediction experiment during 1964–2005. The probability for a random binomial prediction with given value of τ to fall within the shaded area (i.e. to predict more than $N(1-n)$ target earthquakes with given τ) is less or equal than 0.001 (0.1%). The point that corresponds to our experiment is well within this area, thus indicating very high predictive power. It should be emphasized that the results presented in this figure combine the information from the learning period, independent data, and advance prediction (we have too few alarms and target earthquakes during the advance phase to use them alone). Thus, this analysis is not equivalent to evaluating the real predictive power of the algorithm, where only advance results must be used. Nevertheless, the grey shadowed area that corresponds to the binomial model gives a good orientation for the expected significance of the results.

A.7. Significance level: empirical estimation

An alternative approach to testing significance of a prediction algorithm involves empirical estimations of occurrence rate for target earthquakes. Thus, the approach is unavoidably approximate due to the small number of target earthquakes; yet it is much more realistic comparing to the random binomial prediction.

Specifically, we assume that target earthquakes form a Poisson process $N(t,r)$ stationary in time but non-homogeneous in space. The expected number of earthquake within the interval of length t and spatial region R is given by

$$E(N(t,R)) = t\mu(R) \quad \text{(A12)}$$

where $\mu(R)$ is some non-negative measure over the space. In practice, a first-order approximation to this measure can be obtained by considering the number N_R of target earthquakes within the region R per unit of time using observations over S years:

$$\mu(R) \approx N_R/S.$$

With our assumptions, the probability of having exactly k target earthquakes within the region R during time interval of length t is given by Poisson distribution

$$\Pr\{k \text{ target earthquakes within } R\} = \mathrm{e}^{-\mu(R)t}\frac{(\mu(R)t)^k}{k!} \quad \text{(A13)}$$

and the probability p to have at least one target earthquake is

$$p := \Pr\{\text{at least one target earthquake within } R\} = 1-\mathrm{e}^{-\mu(R)t}. \quad \text{(A14)}$$

When the rate of target earthquakes is small (which is indeed the case in our experiment), we can approximate p as

$$p := \Pr\{\text{at least one target earthquake within } R\} \approx \mu(R)t \approx \frac{N_R t}{S} \quad \text{(A15)}$$

Our final goal is to calculate the probability of predicting $N-N_f$ target earthquakes out of N by a set of alarms $A_i=(t_i, R_i)$ that were declared for regions R_i

and time intervals t_i. We denote by p_i the probability to have at least one target earthquake within A_i.

The probability for a given target earthquake to be predicted is calculated as the probability that it will be predicted by at least one of the alarms:

$$\begin{aligned}&\Pr\{\text{given target EQ is predicted}\}\\&= \sum_i \Pr\{\text{given target EQ is within}\, A_i\}\\&= \sum_i \Pr\{\text{given target EQ is within}\, R_i \,\text{during}\, t_i\}\\&= \sum_i \Pr\{\text{given target EQ is within}\, R_i\}\frac{t_i}{T}\\&= \sum_i q_i \frac{t_i}{T}\end{aligned}$$

Here we used the fact that alarms are not overlapping (by definition); factorization property (A12) of the target event process; and the fact that conditional distribution of the occurrence time of an event from Poisson process is uniform, given that this event occurred within the given time interval.

The probability for a given target earthquake to happen within the spatial region R_i can be estimated as

$$q_i = \Pr\{\text{given target EQ happened within } R_i\} = \frac{n_i}{N_\Omega}.$$

where n_i is the number of target earthquakes within R_i during some period S and N_Ω is the total number of target earthquakes within the region Ω considered for prediction during the same time. Finally

$$\begin{aligned}Q :&= \Pr\{\text{given target EQ is predicted}\} \approx \sum_i \frac{n_i}{N_\Omega}\\&\times \frac{t_i}{T} \approx \sum_i p_i \frac{S}{N_\Omega T},\end{aligned}$$

and the distribution of the number of predicted target earthquakes out of N is given by the binomial formula:

$$\begin{aligned}&\Pr\{N - N_f \,\text{out of}\, N \,\text{target EQ are predicted}\}\\&= \binom{N}{N_f} Q^{N-N_f}(1-Q)^{N_f} \approx \binom{N}{N_f}\left(\sum_i \frac{n_i t_i}{N_\Omega T}\right)^{N-N_f}\\&\left(1 - \sum_i \frac{n_i t_i}{N_\Omega T}\right)^{N_f} \approx \binom{N}{N_f}\left(\sum_i p_i \frac{S}{N_\Omega T}\right)^{N-N_f}\\&\left(1 - \sum_i p_i \frac{S}{N_\Omega T}\right)^{N_f}\end{aligned}$$

We apply the above approach to California. Specifically, we consider the region Ω shown in Fig. 2 during the period 1965–2004 (S=40 years); there were N_Ω=10 target earthquakes. The advance prediction was performed within the same region during July 2003–June 2005 (T=2 years), and resulted in three alarms; N=1 target earthquake occurred during this period. The probabilities p_i of having at least one target earthquake within each of the alarms are 5%, 8%, and 5% (see Table 1 and Eq. (A14)). The probability to predict the only target event by chance is estimated as 36%. Notice that this is the conditional probability given the actual number of target earthquakes and alarms. If one does not want to be conditioned by the number of actual target earthquakes, then we need to modify our results using (A13). In the case of California, where we had only one target earthquake, this will give:

$$\begin{aligned}&\Pr\{\text{predict 1 target with our three alarms}\}\\&= \Pr\{\text{there is exactly one target}\}\\&\times \Pr\{\text{it was predicted}\}.\end{aligned}$$

The first probability is estimated using (A13):

$$\begin{aligned}&\Pr\{\text{there is exactly one target}\}\\&= \mu(R)T\mathrm{e}^{-\mu(R)T} \approx \frac{N_\Omega}{S}T\mathrm{e}^{-\frac{N_\Omega}{S}T} = \frac{10}{40}2\mathrm{e}^{-\frac{10}{40}2} \approx 0.3.\end{aligned}$$

Thus, the probability to have only one target event and predict it by chance is approximately $0.36\times 0.3 = 0.12$ (or 12%).

References

Aki, K., Keilis-Borok, V., Gabrielov, A., Jin, A., Liu, Z., Shebalin, P., Zaliapin, I., On the current state of the lithosphere in Central California. Letter with San Simeon prediction sent to a group of leading experts on June 21, 2003. Available at http://www.math.purdue.edu/~agabriel/Workshop/SanSimeon_let.pdf.

ANSS/CNSS Worldwide Earthquake Catalog. (http://quake.geo.berkeley.edu/cnss) (Produced by Advanced National Seismic System (ANSS) and hosted by the Northern California Data Center (NCEDC), 1965–2003).

Bowman, D.D., Ouillon, G., Sammis, C.G., Sornette, A., Sornette, D., 1998. An observational test of the critical earthquake concept. J. Geophys. Res. 103, 24359–24372.

Caputo, M., Console, R., Gabrielov, A.M., Keilis-Borok, V.I., Sidorenko, T.V., 1983. Long-term premonitory seismicity patterns in Italy. Geophys. J. R. Astron. Soc. 75, 71–75.

Daley, D.J., Vere-Jones, D., 2004. Scoring probability forecasts for point processes: the entropy score and information gain. J. Appl. Probab. 41A, 297–312.

De Mare, J., 1980. Optimal prediction of catastrophes with applications to Gaussian processes. Ann. Probab. 8, 841–850.

Gabrielov, A., Keilis-Borok, V., Zaliapin, I., Newman, W.I., 2000. Critical transitions in colliding cascades. Phys. Rev., E 62, 237–249.

Jin, A., Aki, K., Liu, Z., Keilis-Borok, V., 2004. Seismological evidence for the brittle–ductile interaction hypothesis on earthquake loading. Earth Planets Space 56, 823–830.

Jolliffe, I.T., Stephenson, D.B., 2003. Forecast Verification. Wiley, Chichester.

Kadanoff, L.P., 2000. Statistical Physics: Statics, Dynamics, and Renormalization. World Scientific Publishing, Singapore.

Keilis-Borok, V.I., 1990. The lithosphere of the Earth as a non-linear system with implications for earthquake prediction. Rev. Geophys. 28 (1), 19–34.

Keilis-Borok, V., 2002. Earthquake prediction: state-of-the-art and emerging possibilities. Annu. Rev. Earth Planet. Sci. 30, 1–33.

Keilis-Borok, V.I., Shebalin, P.N. (Eds.), 1999. Dynamics of the Lithosphere and Earthquake Prediction, Phys. Earth Planet. Inter. (special issue) vol. 111. , pp. 179–330.

Keilis-Borok, V.I., Soloviev, A.A. (Eds.), 2003. Nonlinear Dynamics of the Lithosphere and Earthquake Prediction. Springer, Heidelberg.

Keilis-Borok, V.I., Knopofff, L., Rotwain, I.M., 1980. Bursts of aftershocks, long-term precursors of strong earthquakes. Nature 283, 259–263.

Keilis-Borok, V., Stock, J.H., Soloviev, A., Mikhalev, P., 2000. Pre-recession pattern of six economic indicators in the USA. J. Forecast. 19, 65–80.

Keilis-Borok, V.I., Shebalin, P.N., Zaliapin, I.V., 2002. Premonitory patterns of seismicity months before a large earthquake: five case histories in Southern California. Proc. Natl. Acad. Sci. 99, 16562–16567.

Keilis-Borok, V., Shebalin, P., Gabrielov, A., Turcotte, D., 2004. Reverse tracing of short-term earthquake precursors. Phys. Earth Planet. Inter. 145, 75–85.

Knopoff, L., Levshina, T., Keilis-Borok, V.I., Mattoni, C., 1996. Increased long-range intermediate-magnitude earthquake activity prior to strong earthquakes in California. J. Geophys. Res. 101, 5779–5796.

Lindgren, G., 1975. Prediction from a random time point. Ann. Probab. 3, 412–423.

Lindgren, G., 1985. Optimal prediction of level crossings in Gaussian processes and sequences. Ann. Probab. 13, 804–824.

Ma, Z., Fu, Z., Zhang, Y., Wang, C., Zhang, G., Liu, D., 1990. Earthquake Prediction: Nine Major Earthquakes in China. Springer-Verlag, New York.

Mogi, K., 1981. Seismicity in Western Japan and long-term forecasting. Earthquake Prediction: an International Review, Maurice Ewing Series, vol. 4. American Geophysical Union, Washington, DC, pp. 43–51.

Molchan, G.M., 1990. Strategies in strong earthquake prediction. Phys. Earth Planet. Inter. 61 (1–2), 84–98.

Molchan, G.M., 2003. Earthquake prediction strategies: a theoretical analysis. In: Keilis-Borok, V.I., Soloviev, A.A. (Eds.), Nonlinear Dynamics of the Lithosphere and Earthquake Prediction. Springer, Heidelberg, pp. 209–237.

Molchan, G.M., Dmitrieva, O.E., Rotwain, I.M., Dewey, J., 1990. Statistical analysis of the results of earthquake prediction, based on burst of aftershocks. Phys. Earth Planet. Inter. 61, 128–139.

Prozorov, A.G., Schreider, S.Yu., 1990. Real time test of the long-range aftershock algorithm as a tool for mid-term earthquake prediction in Southern California. Pure Appl. Geophys. 133, 329–347.

Rundle, J.B., Turcotte, D.L., Shcherbakov, R., Klein, W., Sammis, C., 2003. Statistical physics approach to understanding the multiscale dynamics of earthquake fault systems. Rev. Geophys. 41, 1019.

Rundquist, D.V., Soloviev, A.A., 1999. Numerical modeling of block structure dynamics: an arc subduction zone. Phys. Earth Planet. Inter. 111, 241–252.

Shebalin, P., Zaliapin, I., Keilis-Borok, V.I., 2000. Premonitory rise of the earthquakes' correlation range: lesser Antilles. Phys. Earth Planet. Inter. 122, 241–249.

Shebalin, P., Keilis-Borok, V.I., Zaliapin, I., Uyeda, S., Nagao, T., Tsybin, N., 2003. Short-term Premonitory Rise of the Earthquake Correlation Range//IUGG2003, June 30–July 11, 2003, Sapporo, Japan. Abstracts. A184.

Shebalin, P., Keilis-Borok, V., Zaliapin, I., Uyeda, S., Nagao, T., Tsybin, N., 2004. Advance short-term prediction of the large Tokachi-Oki earthquake, September 25, 2003, $M=8.1$: a case history. Earth Planets Space 56, 715–724.

Simons, M., Fialko, Y., Rivera, L., 2002. Coseismic deformation from the 1999 M_W 7.1 Hector Mine, California, earthquake as inferred from InSAR and GPS observations. Bull. Seismol. Soc. Am. 92, 1390–1402.

Sykes, L.R., 1983. Predicting great earthquakes. In: Kanamori, H., Boschi, E. (Eds.), Earthquakes, Observation, Theory, and Interpretation. North Holland, New York, pp. 398–435.

Uyeda, S., Park, S. (Eds.), 2002. Proceedings of the International Symposium on The Recent Aspects of Electromagnetic Variations Related with Earthquakes, 20 and 21 December 1999, J. Geodyn., vol. 33, pp. 4–5. Special issue.

Whittle, P., 1963. Prediction and Regulation by Linear Least-Squares Methods. English University Press, London.

Zaliapin, I., Keilis-Borok, V.I., Axen, G., 2002. Premonitory spreading of seismicity over the faults' network in southern California: precursor accord. J. Geophys. Res., B 107, 2221.

Zaliapin, I., Keilis-Borok, V.I., Ghil, M., 2003. A Boolean delay equation model of colliding cascades. Part II. Prediction of critical transitions. J. Stat. Phys. 111, 839–861.

Zöller, G., Hainzl, S., 2001. Detecting premonitory seismicity patterns based on critical point dynamics. Nat. Hazards Earth Syst. Sci. 1, 93–98.

Zöller, G., Hainzl, S., Kurths, J., 2001. Observation of growing correlation length as an indicator for critical point behavior prior to large earthquakes. J. Geophys. Res. 106, 2167–2176.